ORNL/TM-2016/537

Independent Modeling of the Alkali-Silica Reaction: Mock-up Test Block

Mohammad A. Hariri-Ardebili
Victor E. Saouma
Yann LePape

Date: Sept. 15, 2016

OAK RIDGE NATIONAL LABORATORY
MANAGED BY UT-BATTELLE FOR THE US DEPARTMENT OF ENERGY

DOCUMENT AVAILABILITY

Reports produced after January 1, 1996, are generally available free via US Department of Energy (DOE) SciTech Connect.

Website: `http://www.osti.gov/scitech/`

Reports produced before January 1, 1996, may be purchased by members of the public from the following source:

National Technical Information Service
5285 Port Royal Road
Springfield, VA 22161
Telephone: 703-605-6000 (1-800-553-6847)
TDD: 703-487-4639
Fax: 703-605-6900
E-mail: info@ntis.fedworld.gov
Website: `http://www.ntis.gov/help/ordermethods.aspx`

Reports are available to DOE employees, DOE contractors, Energy Technology Data Exchange representatives, and International Nuclear Information System representatives from the following source:

Office of Scientific and Technical Information
PO Box 62
Oak Ridge, TN 37831
Telephone: 865-576-8401
Fax: 865-576-5728
E-mail: report@osti.gov
Website: `http://www.osti.gov/contact.html`

This report was prepared as an account of work sponsored by an agency of the United States Government. Neither the United States Government nor any agency thereof, nor any of their employees, makes any warranty, express or implied, or assumes any legal liability or responsibility for the accuracy, completeness, or usefulness of any information, apparatus, product, or process disclosed, or represents that its use would not infringe privately owned rights. Reference herein to any specific commercial product, process, or service by trade name, trademark, manufacturer, or otherwise, does not necessarily constitute or imply its endorsement, recommendation, or favoring by the United States Government or any agency thereof. The views and opinions of authors expressed herein do not necessarily state or reflect those of the United States Government or any agency thereof.

ORNL/TM-2016/537

Division or Program Name

Independent Modeling of the Alkali-Silica Reaction: Mock-up Test Block

Mohammad Amin Hariri-Ardebili
Victor E. Saouma
Yann LePape

September 2016
University of Colorado, Boulder CO 80309-0428

OAK RIDGE NATIONAL LABORATORY
P.O. Box 2008
Oak Ridge, Tennessee 37831-6285
managed by
UT-Battelle, LLC
for the
US DEPARTMENT OF ENERGY
under contract DE-AC05-00OR22725

CONTENTS

Page

LIST OF FIGURES . . . vi
LIST OF TABLES . . . vii

1 Problem Description **1**
1.1 Objective . . . 1
1.2 Test Description . . . 1
1.2.1 Geometry . . . 1
1.3 Material properties . . . 3
1.3.1 Target mix design . . . 3
1.3.2 Mechanical properties . . . 3
1.3.3 Test duration and projected free expansion . . . 3
1.3.3.1 Expansion curves . . . 4

2 Model preparation **6**
2.1 Units . . . 6
2.2 Finite element model . . . 6
2.3 Material properties . . . 8
2.4 Expansion curves . . . 9
2.5 Output data; Recoders location . . . 13
2.6 Analysis Procedure . . . 18
2.7 Generated Data . . . 18

3 Result **21**
3.1 Deterministic results . . . 22
3.2 Probabilistic Based Predictions . . . 23
3.2.1 Concrete Strains and Stress Histograms . . . 23
3.2.2 DEMEC . . . 37
3.2.3 Displacements . . . 39
3.2.4 Reinforcements Stress and Strains . . . 40
3.3 Conclusions . . . 45

A Data Base & `P5.m` **47**

LIST OF FIGURES

Figures **Page**

1.1 Specimens 2
1.2 Stress Strain curve (28 days) 4
1.3 Concrete expansion block tested by Prof. E. Giannini 4
1.4 Laboratory measured expansion 5

2.1 Geometry model of quarter block with boundary conditions 6
2.2 Finite element mesh of the quarter model 7
2.3 Kinetic curve for the ASR expansion 11
2.4 Random generation of expansion curves based on present and future uncertainties. 11
2.5 Sensors physical and numerical locations 15
2.6 Locations of sensors and data point recorders in the finite element mesh 16
2.7 Location of reinforcement strain gages and recorders 17
2.8 File generation algorithm 18
2.9 Standard deviation *vs.* percentile definition for normal distribution 19

3.1 Selected views of deformed shapes; contour lines correspond to vertical displacement and crack pattern 21
3.2 Stresses and AAR strains at the top center node 22
3.3 Stress & Strains at Locator # 1, DOF = 3, Coordinates (m)<0.8382, 0.5842, 0.508> 24
3.4 Stress & Strains at Locator # 2, DOF = 3, Coordinates (m)<1.6002, 0.5842, 0.508> 24
3.5 Stress & Strains at Locator # 3, DOF = 3, Coordinates (m)<1.0922, 0.8382, 0.508> 25
3.6 Stress & Strains at Locator # 4, DOF = 3, Coordinates (m)<1.3462, 1.0922, 0.254> 25
3.7 Stress & Strains at Locator # 5, DOF = 3, Coordinates (m)<1.3462, 1.0922, 0.508> 26
3.8 Stress & Strains at Locator # 6, DOF = 3, Coordinates (m)<1.3462, 1.0922, 0.762> 26
3.9 Stress & Strains at Locator # 7, DOF = 3, Coordinates (m)<1.6002, 1.0922, 0.508> 27
3.10 Stress & Strains at Locator # 8, DOF = 3, Coordinates (m)<0.8382, 1.3462, 0.508> 27
3.11 Stress & Strains at Locator # 9, DOF = 3, Coordinates (m)<1.3462, 1.3462, 0.508> 28
3.12 Stress & Strains at Locator # 10, DOF = 3, Coordinates (m)<1.6002, 1.3462, 0.254> 28
3.13 Stress & Strains at Locator # 11, DOF = 3, Coordinates (m)<1.6002, 1.3462, 0.508> 29
3.14 Stress & Strains at Locator # 12, DOF = 3, Coordinates (m)<1.6002, 1.3462, 0.762> 29
3.15 Stress & Strains at Locator # 13, DOF = 1, Coordinates (m)<0.9652, 1.0922, 0.3048> 30
3.16 Stress & Strains at Locator # 14, DOF = 1, Coordinates (m)<0.9652, 1.0922, 0.7112> 31
3.17 Stress & Strains at Locator # 15, DOF = 1, Coordinates (m)<1.2192, 0.5842, 0.3048> 31
3.18 Stress & Strains at Locator # 16, DOF = 1, Coordinates (m)<1.2192, 0.5842, 0.7112> 32
3.19 Stress & Strains at Locator # 17, DOF = 1, Coordinates (m)<1.4732, 1.3462, 0.3048> 32

3.20 Stress & Strains at Locator # 18, DOF = 1, Coordinates (m)<1.4732, 1.3462, 0.7112> 33
3.21 Stress & Strains at Locator # 19, DOF = 2, Coordinates (m)<1.6002, 0.7112, 0.3048> 33
3.22 Stress & Strains at Locator # 20, DOF = 2, Coordinates (m)<1.6002, 0.7112, 0.7112> 34
3.23 Stress & Strains at Locator # 21, DOF = 2, Coordinates (m)<0.8382, 0.9652, 0.3048> 34
3.24 Stress & Strains at Locator # 22, DOF = 2, Coordinates (m)<0.8382, 0.9652, 0.7112> 35
3.25 Stress & Strains at Locator # 23, DOF = 2, Coordinates (m)<1.6002, 1.2192, 0.3048> 35
3.26 Stress & Strains at Locator # 24, DOF = 2, Coordinates (m)<1.6002, 1.2192,0.7112> 36
3.27 Demec Reading # 1; Between <1.004273, 0.761996, 1.016> and <1.727196, 0.761996, 1.016> 37
3.28 Demec Reading # 2; Between <1.004273, 0.761996, 1.016> and <1.004273, 1.473196, 1.016> 37
3.29 Demec Reading # 3; Between <1.004273, 1.473196, 1.016> and <1.727196, 1.473196, 1.016> 38
3.30 Demec Reading # 4; Between <1.727196, 0.761996, 1.016> and <1.727196, 1.473196, 1.016> 38
3.31 Vertical displacement of top center point. 39
3.32 Vertical displacement of bottom center point. 39
3.33 Reinforcement stress and strain at Locator # 1;<1.632, 1.378, 0.0953> 40
3.34 Reinforcement stress and strain at Locator # 2;<2.14, 1.886, 0.0953> 41
3.35 Reinforcement stress and strain at Locator # 3;<1.632, 1.378, 0.9208> 41
3.36 Reinforcement stress and strain at Locator # 4;<2.14, 1.886, 0.9208> 42
3.37 Reinforcement stress and strain at Locator # 5;<1.632, 1.378, 0.1334> 42
3.38 Reinforcement stress and strain at Locator # 6;<2.14, 1.886, 0.1334> 43
3.39 Reinforcement stress and strain at Locator # 7;<1.632, 1.378, 0.8827> 43
3.40 Reinforcement stress and strain at Locator # 8;<2.14, 1.886, 0.8827> 44

LIST OF TABLES

Tables **Page**

1.1 Characteristics of the three specimens 1
1.2 Target mix design 3
1.3 Reported 28 days compressive strengths f_c' (MPa) 3
1.4 Reported 28 days tensile strengths f_t' (MPa) 3
1.5 Reported 28 days elastic modulus (GPa) 4
1.6 Provided expansion curve data 5

2.1 Concrete input paramters 8
2.2 ASR input parameters 9
2.3 Correlation between concrete input paramters 10
2.4 Correlation between AAR input parameters 10
2.5 Strain gages location points, and corresponding closest Merlin nodes 13
2.6 Demec location points, and corresponding closest Merlin nodes 14
2.7 Numerical gages in Merlin 14
2.8 Coordinates of the vertical displacement recorders (m) 14
2.9 Location of reinforcement strain gages 16
2.10 Generated random variables based on LHS 19

Chapter 1

Problem Description

Data in this section were provided either by Prof. E. Giannini (University of Alabama) or Prof. Z.J. Ma (University of Tennessee).

1.1 OBJECTIVE

The University of Tennessee (Knoxville), under DOE contract M2LW-16OR0403014 will be performing large scale laboratory test of confined and unconfined concrete blocks (simulating a nuclear class-I safety reinforced concrete structure) to complement the test results of Multon et al. (2008) (obtained on a much smaller scale and large-scale testing conducted at the University of Texas, Austin and at the National Institute of Standards and Technology).

Parallel to this effort, the University of Colorado at Boulder is under contract to perform predictive numerical simulations of those tests in order to anticipate test results.

1.2 TEST DESCRIPTION

1.2.1 GEOMETRY

As part of a research to quantify the effect of confinement on expanding concrete due to alkali-silica reaction (ASR), reactive concrete is cast inside a rigid confining frame (CASR) while a similar concrete block is allowed to freely expand (UASR), table 1.1. There is also a control specimen (Cont).

Specimens, $116'' \times 136'' \times 40''$, fig. 1.1 have two layers of 22 # 11 bars (1.41" diameter) (10 in one direction and 12 in another one) each, fig. 1.1(d).

Soon after casting 2 dywidag rod (diameters $2.5''$) provide additional lateral restrain to the confined mockup. It is initially just slightly tightened to avoid "slack".

Table 1.1. Characteristics of the three specimens

ID	Label	Confined	Reactive
1	CASR	Yes	Yes
2	UASR	No	Yes
3	Cont	No	No

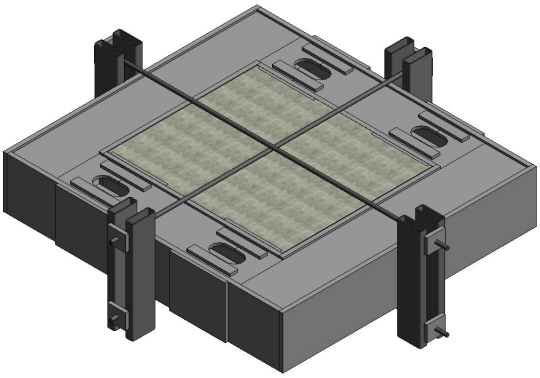

(a) Computer rendering

(b) Form construction

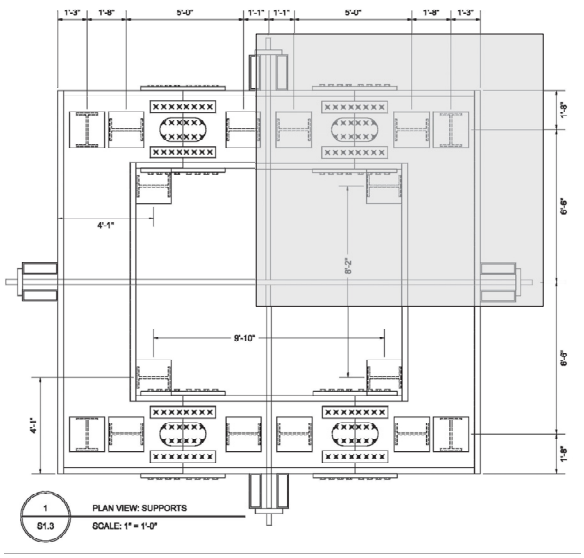

(c) Specimen dimensions (Shaded area will be numerically modeled)

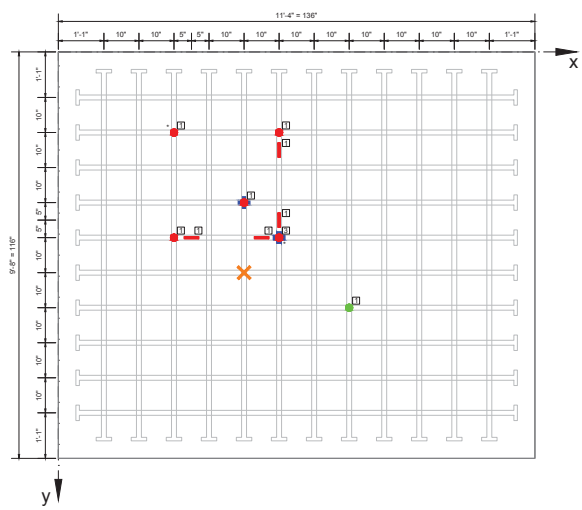

(d) Configuration of the reinforcement in the concrete block

Fig. 1.1. Specimens

A few days after casting, the bottom support is removed, and the concrete block is vertically supported by four 18″ × 18″ corner plates.

Following casting, specimens have been stored at 38°C and about 95%RH for about three years inside an environmental chamber.

1.3 MATERIAL PROPERTIES

1.3.1 TARGET MIX DESIGN

Mix design has been extensively investigated at the University of Alabama, and the one retained is shown in table 1.2 with 1" maximum size aggregate (MSA) composed of Green schist - muscovite, chlorite, quartz, Na-feldspar, K-feldspar, calcite, cristobalite.

In this mix, only the coarse aggregate is reactive, the fine is not. This will have the effect of "slowing" the reaction.

Table 1.2. Target mix design

Component	Kg/m^3
Coarse aggregates	1,180
Fine aggregates	757
Cement	350
Water	158
w/c	0.45
50% NaOH solution	9.4

1.3.2 MECHANICAL PROPERTIES

28 days mechanical properties, compressive and tensile strengths, and the elastic modulus are shown in table 1.3, table 1.4 and table 1.5, respectively along with their mean and standard deviations.

Table 1.3. Reported 28 days compressive strengths f_c' (MPa)

Specimen Type	Cyl 1	Cyl 2	Cyl 3	Cyl 4	Cyl 5	AVG	STD
CASR	17.5	18.3	24.0	22.6	19.9	20.4	2.78
UASR	19.0	21.0	19.2	19.3	21.6	20.0	1.20

CASR: Confined Reactive Specimen

UASR: Unconfined Reactive Specimen

Table 1.4. Reported 28 days tensile strengths f_t' (MPa)

Specimen Type	Cyl	Cyl	AVG	STD
CASR	2.85	2.55	2.70	0.215
UASR	2.10	2.16	2.13	0.044

CASR: Confined Reactive Specimen

UASR: Unconfined Reactive Specimen

A representative 28 days stress-strain curve is shown in fig. 1.2.

1.3.3 TEST DURATION AND PROJECTED FREE EXPANSION

Casting occurred early July 2015, and a desired prediction for April 30 2019 is required. Hence, the prediction should span 34 months (148 weeks or 1,030 days). The projected maximum expansion is 6.7%

Table 1.5. Reported 28 days elastic modulus (GPa)

Specimen Type	Cyl	Cyl	AVG	STD
CASR	26.9	22.8	24.9	2.91
UASR	23.8	26.4	25.1	1.80

CASR: Confined Reactive Specimen

UASR: Unconfined Reactive Specimen

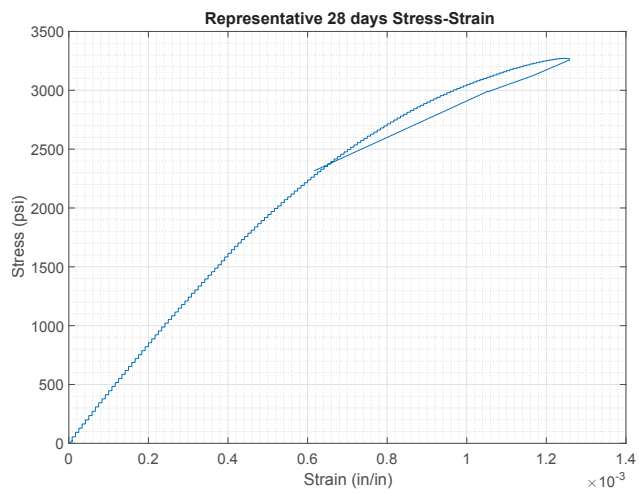

Fig. 1.2. Stress Strain curve (28 days)

(0.0067).

1.3.3.1 Expansion curves

Expansion curves were obtained by Prof. E. Giannini from (300 × 300 × 600 mm) specimens stored at 38°C and 95%RH shown in fig. 1.3.

Fig. 1.3. Concrete expansion block tested by Prof. E. Giannini

Data are tabulated in table 1.6 and shown in fig. 1.4 where the vertical expansions are taken over a 150 mm gauge length, and the longitudinal ones (same direction as longitudinal) are taken over a 500 mm gauge length. It should be noted that the reported mean (or average) corresponds to the average of all the

experimental values.

Table 1.6. Provided expansion curve data

Calculated Expansions							
Age	Top		Sides				
(Days)	Long	Trans	Longitudinal	Longitudinal	Vertical	Vertical	Average
6	0.000%	0.000%	0.000%	0.000%	0.000%	0.000%	**0.000%**
40	-0.006%	-0.007%	-0.003%	-0.009%	0.004%	-0.005%	**-0.004%**
68	-0.001%	-0.002%	0.002%	-0.001%	0.006%	-0.002%	**0.000%**
87	0.007%	0.009%	0.009%	0.007%	0.028%	0.010%	**0.012%**
103	0.015%	0.016%	0.014%	0.014%	0.037%	0.023%	**0.020%**
117	0.023%	0.022%	0.023%	0.021%	0.048%	0.028%	**0.028%**
138	0.035%	0.034%	0.033%	0.033%	0.079%	0.059%	**0.045%**
152	0.044%	0.042%	0.041%	0.041%	0.100%	0.076%	**0.057%**
170	0.054%	0.051%	0.048%	0.052%	0.122%	0.094%	**0.070%**
190	0.066%	0.062%	0.062%	0.065%	0.149%	0.123%	**0.088%**
220	0.079%	0.073%	0.073%	0.077%	0.175%	0.141%	**0.103%**

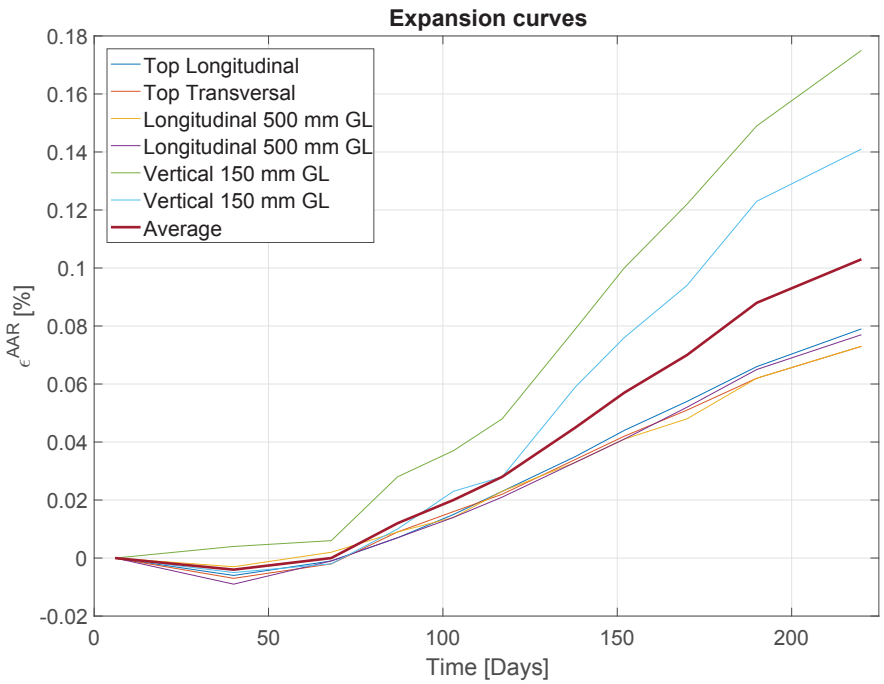

Fig. 1.4. Laboratory measured expansion

Chapter 2

Model preparation

Following description of the test (with data externally provided), this chapter details the interpretation of these data into a numerical model for a probabilistic based simulation that will enable proper long term prediction.

2.1 UNITS

Units used in all calculations are m, sec, MN, and MPa.

2.2 FINITE ELEMENT MODEL

Given the double symmetry in the model, numerical model considered only a quarter of the block (though randomness of the actual material properties could preclude such a simplification if it was also modeled). fig. 2.1 schematically illustrates the simplified numerical model. Different material/loading parts are shown in different colors.

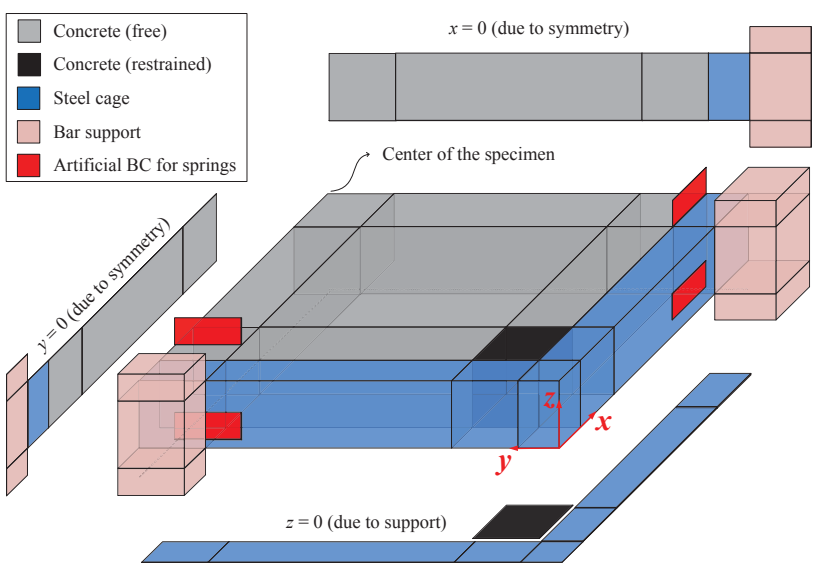

Fig. 2.1. Geometry model of quarter block with boundary conditions

The model is composed of the following components: concrete (gray), steel cage (blue), and Diwydag anchors (pink). Also shown are the boundary conditions that exploit the double symmetry.

Given the complexity of the confinement steel frame (CSF), and without any anticipated loss in accuracy, the web/flange based CSF are replaced by an equivalent solid block (fig. 2.1 in blue). The block will have a flexural stiffness (EI) equal to the one of the web/flange actual CSF the moment inertia of which (determined by the UT team) is 101,972 in^4 or 0.0424 m^4. Thus, an equivalent EI section is determined to be 31.26″ or 0.794 m wide.

$$I = \frac{bh^3}{12} = \frac{1.016 \times 0.794^3}{12} = 0.0424 \text{ m}^4 \tag{2.1}$$

Then fig. 2.2 shows the finite element mesh where the red part corresponding to the Dywidag supports. Also shown is the reinforcement within the concrete fig. 2.2(b). Note that the reinforcement is modeled as smeared within the concrete elements (i.e. one simply needs to specifies the coordinates of the first and end point of each rebar).

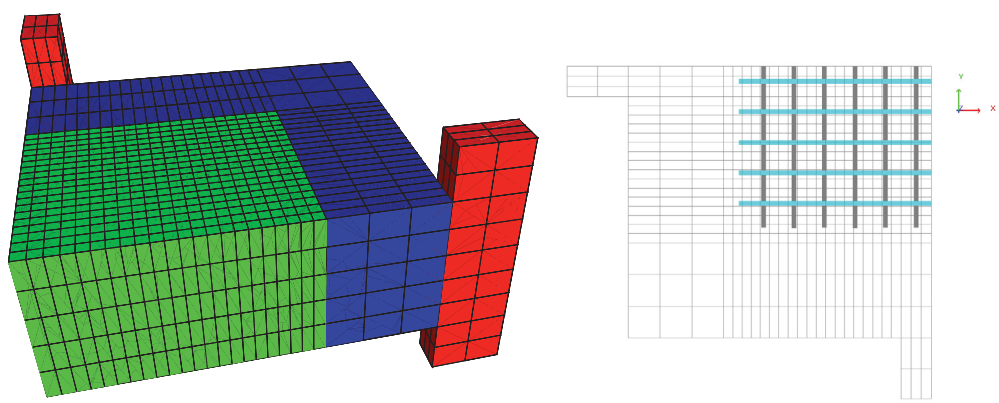

(a) Different material group (b) Reinforcement

Fig. 2.2. Finite element mesh of the quarter model

Modeling of the dywidag is done by a spring connected to the end of the vertical clamp. For THREADBARS®, The modulus of elasticity is 205 MPa (or MN/m^2) (29,700 ksi). The reported diameter is 66 mm with a reported cross sectional area of 3,331 mm^2. The length of the bars are 16’ 4” and 18”. For the sake of simplicity an average length of 17.15’ is taken or 5.2 m. Finally, since one quarter of the plate is modeled, the cross sectional area is reduced by half to 1,665 mm^2. Hence the spring stiffness can be readily computed as:

$$k_{sp} = \frac{AE}{L} = \frac{(1,665 \times 10^{-6})\text{m}^2\ (205)\text{MN/m}^2}{(5.2)\text{m}} = 0.066\text{MN/m} \tag{2.2}$$

Contact between the concrete and the confining steel cage was modeled as a perfect one. This important assessment is based on the high interface stresses between the two materials once the concrete expands and their high coefficient of friction. Furthermore, it is well known that in cylinder compressive strength tests, unless special measures are taken, the testing equipment plates do provide full lateral confinement (which greatly affect the failure mode of the cylinder).

2.3 MATERIAL PROPERTIES

A purely deterministic prediction for such a complex experimental setup, with many poorly quantified parameters (such as the kinetics of the expansion), is nearly impossible. Henceforth, a more rational one is to assume probability distribution function for the material properties. More specifically truncated normalized standard distributions are considered. Those are characterized by a mean, standard deviation, upper and lower bounds. Hence, material properties are shown in table 2.1 for the linear/nonlinear concrete model, and table 2.2 for the ASR model, where:

COV Coefficient of variation ($\frac{mean}{STD}$)
Active A flag, 0: Deterministic; 1: Probabilistic
STD Computed standard deviation
BL Bound limits
LB Lower bound (Mean-BL)
UB Upper bound (Mean+BL)

Note that values in red correspond to material properties obtained from laboratory tests (such as compressive strength) or directly derived from them (such as the fracture energy). All others are best estimates based on the authors experience.

Table 2.1. Concrete input paramters

Property	RV_{ID}	Unit	Mean	COV	Active	STD	BL	LB	UB
Thickness	1	m	1	0.2	0	0	0.5	0	0
Mass density	2	Gg/m3	2.25E-03	0.2	0	0	0.5	0	0
Coefficient of thermal expansion	3	1/Cô	9.90E-06	0.2	0	0	0.5	0	0
Elastic/Young's modulus	4	MPa	24,900	0.12	1	2,988	0.25	18,675	31,125
Poisson's ratio	5	-	0.2	0.2	0	0	0.5	0	0
Tensile strength	6	MPa	2.7	0.08	1	0.216	0.3	1.89	3.51
Gf - Exponential softening	7	MN/m	9.50E-05	0.3	1	2.85E-05	0.4	5.70E-05	1.33E-04
Compressive strength	8	MPa	-20.4	0.14	1	2.856	0.25	-25.5	-15.3
Compressive critical displacement	9	m	-5.00E-04	0.2	0	0	0.5	0	0
Factor beta for return direction	10	-	0	0.2	0	0	0.5	0	0
Factor e for roundness of failure surface	11	-	0.6	0.15	1	0.09	0.2	0.51	0.99
Onset of nonlinearity in compression	12	MPa	-20	0.05	0	1	0.2	0	0
Plastic strain at compressive stresngth	13	-	-1.00E-03	0.2	0	0	0.5	0	0

The steel box is assigned an elastic modulus of 200,000 MPa, a Poisson ratio of 0.3. Self weight is ignored.

The dywidag rebar has a cross sectional area of 0.003165 m^2, an elastic modulus of 200,000 MPa, a Poisson ratio of 0.3, and a yield stress of 248 MPa.

Using extensive nonlinear optimization studies based on the Levenberg-Marquardt algorithm, Bažant and Becq-Giraudon (2001) obtained two simple approximate formula for the means of G_F (N/m) as

Table 2.2. ASR input parameters

Property	RV_{ID}	Unit	Mean	COV	Active	STD	BL	LB	UB
Model No.	1	-	2	-	0	0	-	0	0
Maximum volumetric strain	2	-	Refer to fig. 2.4						
Characteristic time	3	ATU	Refer to fig. 2.4						
Latency time	4	ATU	Refer to fig. 2.4						
Activation energy for char	5	^{o}K	5,400	0.8	1	4,320	0.1	4,860	5,940
Activation energy for lat	6	^{o}K	9,400	0.8	1	7,520	0.1	8,460	10,340
Residual red. Factor tension	7	-	0.5	0.2	1	0.1	0.33	0.335	0.665
Fraction of tension pre-AAR	8	-	0.5	0.2	1	0.1	0.4	0.3	0.7
Compressive strength	9	MPa	Refer to table 2.1						
Tensile strength	10	MPa	Refer to table 2.1						
Shape factor for Gamma_c	11	-	-2	0.2	0	0	0.5	0	0
Reference temperature test	12	^{o}C	38.0	0.2	0	0	0.85	0	0
Upper comp. stress limit	13	MPa	-8.00	0.2	0	0	0.5	0	0
Reduction factor Young	14	-	0.6	0.8	1	0.48	0.2	0.48	0.72
Reduction factor tensile	15	-	0.6	0.8	1	0.48	0.2	0.48	0.72

functions of the compressive strength f'_c (MPa), maximum aggregate size d_a (mm), water-cement ratio w/c, and shape of aggregate (crushed or river):

$$G_F = 2.5\alpha_0 \left(\frac{f'_c}{0.051}\right)^{0.46} \left(1 + \frac{d_a}{11.27}\right)^{0.22} \left(\frac{w}{c}\right)^{-0.30} \qquad \omega_{G_F} = 29.9\% \tag{2.3}$$

$$\tag{2.4}$$

where $\alpha_0 = \gamma_0 = 1$ for rounded aggregates, while $\alpha_0 = 1.44$ and $\gamma_0 = 1.12$ for crushed or angular aggregates; ω_{G_F} is the coefficients of variation of the ratios G_F^{test}/G_F, for which a normal distribution may be assumed. Note that this value will be used later for the normal distribution of G_F. Substituting

$$G_F = \frac{(2.5)(1.44)}{10^6} \left(\frac{20.4}{0.051}\right)^{0.46} \left(1 + \frac{25.4}{11.27}\right)^{0.22} (0.45)^{-0.30} = 9.33 \times 10^{-5} \text{MN/m} \tag{2.5}$$

In the analysis, not all material properties are entirely independent. Inter-relationship is best characterized by co-varaince (a metric on how much two random variables change together). Adopted covariances for concrete and AAR are tabulated in table 2.3 and table 2.4. A weak covariance was arbitrarily assigned a value of 0.3, and a strong one a value of 0.7. The absence of any correlation results in a covariance of zero.

All the above data are properly stored in an Excel file for subsequent use by `p1.m` (explained below).

2.4 EXPANSION CURVES

Prediction of future expansion and accompanying strains/displacements is critically dependent on the kinetic curve assigned to the model. A widely accepted one, is the kinetic expansion proposed by Larive (1998):

$$\xi(t, \theta) = \frac{1 - e^{-\frac{t}{\tau_c(\theta)}}}{1 + e^{-\frac{(t-\tau_l(\theta))}{\tau_c(\theta)}}} \tag{2.6}$$

where τ_l and τ_c are the latency and characteristic times respectively. The first corresponds to the inflexion point, and the second is defined in terms of the intersection of the tangent at τ_L with the asymptotic unit

Table 2.3. Correlation between concrete input paramters

Property	RVid	1	2	3	4	5	6	7	8	9	10	11	12	13
Thickness	1	1												
Mass density	2	0	1											
Coefficient of thermal expansion	3	0	0	1										
Elastic/Young's modulus	4	0	0	0	1									
Poisson's ratio	5	0	0	0	0	1								
Tensile strength	6	0	0	0	0	0	1							
G_F - Exponential softening	7	0	0	0	0	0	0.5	1						
Compressive strength (must be negative)	8	0	0	0	0.5	0	0	0	1					
Compressive critical displacement	9	0	0	0	0	0	0.7	0	0	1				
Factor beta for return direction	10	0	0	0	0	0	0	0	0	0	1			
Factor e for roundness of failure surface	11	0	0	0	0	0	0	0	0	0	0	1		
Onset of nonlinearity in compression	12	0	0	0	0	0	0	0	0	0	0	0	1	
Plastic strain at compressive stresngth	13	0	0	0	0	0	0	0	0	0	0	0	0	1

Table 2.4. Correlation between AAR input parameters

Property	RVid	1	2	3	4	5	6	7	8	9	10	11	12	13	14	15
Model No.	1	1														
Maximum volumetric strain	2	0	1													
Characteristic time	3	0	0	1												
Latency time	4	0	0	0.5	1											
Activation energy for char	5	0	0	0	0	1										
Activation energy for lat	6	0	0	0	0	0.7	1									
Residual red. Factor tension	7	0	0	0	0	0	0	1								
Fraction of tension pre-AAR	8	0	0	0	0	0	0	0	1							
Compressive strength	9	0	0	0	0	0	0	0	0	1						
Tensile strength	10	0	0	0	0	0	0	0	0	0.5	1					
Shape factor for Gamma_c	11	0	0	0	0	0	0	0	0	0	0	1				
Reference temperature test	12	0	0	0	0	0	0	0	0	0	0	0	1			
Upper comp. stress limit	13	0	0	0	0	0	0	0	0	0	0	0	0	1		
Reduction factor Young	14	0	0	0	0	0	0	0	0	0	0	0	0	0	1	
Reduction factor tensile	15	0	0	0	0	0	0	0	0	0	0	0	0	0	0	1

value of ξ, fig. 2.3(a). A physical interpretation of the expansion curve was provided by Saouma et al. (2015) and is schematically shown in fig. 2.3(b).

The latency time τ_l and characteristic time τ_c are given by:

$$\begin{aligned} \tau_l(\theta) &= \tau_l(\theta_0)\exp\left[U_l\left(\frac{1}{\theta}-\frac{1}{\theta_0}\right)\right] \\ \tau_c(\theta) &= \tau_c(\theta_0)\exp\left[U_c\left(\frac{1}{\theta}-\frac{1}{\theta_0}\right)\right] \end{aligned} \tag{2.7}$$

expressed in terms of the absolute temperature ($\theta^o K = 273 + T^o C$) and the corresponding activation energies. U_l and U_c are the activation energies minimum energy required to trigger the reaction for the latency and characteristic times respectively.

Based on the above, the key question is how to assign expansion curves in the context of a probabilistic based investigation. With reference to fig. 2.4:

Given the following observations

1. The laboratory measured mean expansion after 200 days, fig. 1.4.

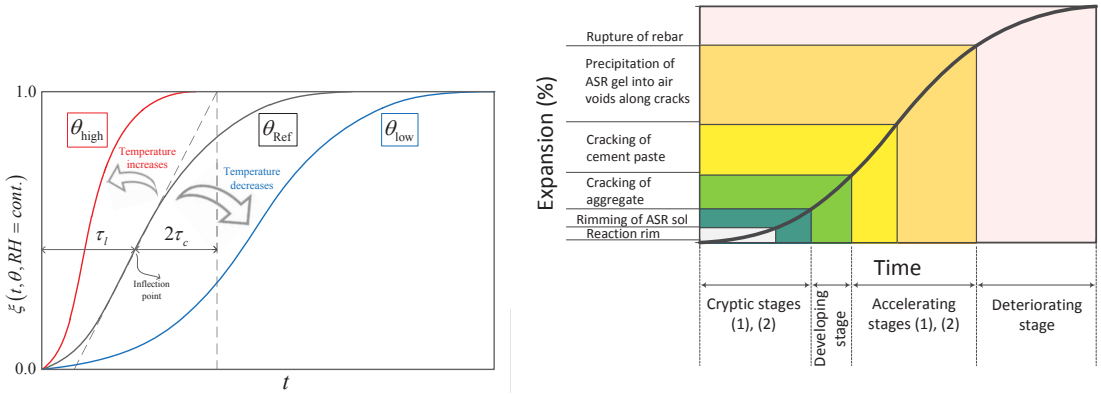

(a) Normalized kinetic curve highlighting effect of temperature

(b) Physical deterioration associated with expansion (Saouma et al. 2015)

Fig. 2.3. Kinetic curve for the ASR expansion

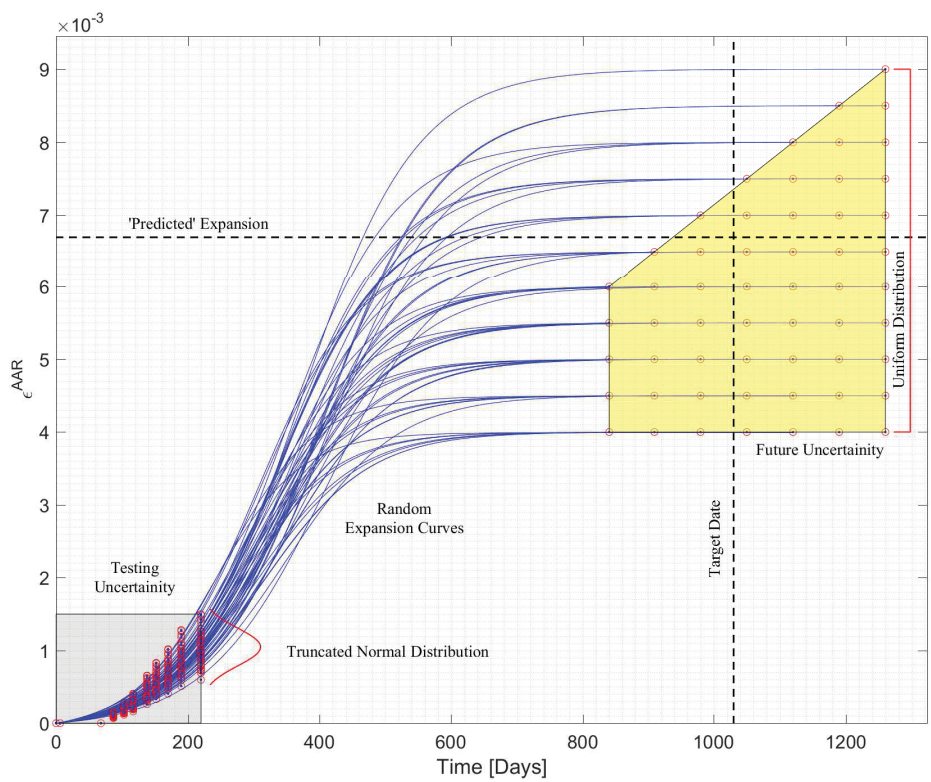

Fig. 2.4. Random generation of expansion curves based on present and future uncertainties.

2. The prediction to be made for April 30, 2019 (1,030 days, 34 months).

3. The anticipated (as reported to the project) maximum expansion will be 6.7%
4. There is obviously an uncertainty as to when the maximum expansion will be reached.

Define uncertainty parameters for the analyses:

1. A truncated normal distribution at 200 days expansion. For the current uncertainty a mean value vector for the reported 200 days (last column in table 1.6) was defined. The (arbitrarily) assigned coefficient of variation was 0.25 (i.e. $\sigma = 0.25\mu$). The cutoff points were set to 0.5 of the corresponding mean value.
2. A uniform distribution for the expansion at age 1.030 days was assumed and "wrapped" around the anticipated one of 6.7%.
3. Given the temporal uncertainty a bracket of 840 (near future) and 1,260 (far future) days was assumed.
4. AAR uncertainty was assumed to be 4 to 6 percent expansion at 840 days, and 4 to 9 percent at 1,260 days. Hence the future uncertainty domain is trapezoidal.
5. Based on the above, the following methodology was followed and implemented in `P1.m` (described below).

Compute the uncertainty curves for each of the simulations:

1. Time and AAR density variations were selected. More specifically time was partitioned in 6, near expansion in 4 and the future one in 10. This results in a total of 56 points uniformly distributed within the future uncertainty domain.
2. Each one of the 56 points will be separately sampled in the spirit of the Latin Hypercube sampling (LHS) wise methodology (Iman and Conover 1982).
3. Separately, generate 56 random truncated expansion curves (from time zero to 200 days) for the current uncertainty domain.
4. Generate 56 full expansion curves as follows:
   (a) Randomly select one of the 56 truncated curves, and a random point inside the future uncertainty domain.
   (b) Using an optimization procedure, fit a continuous curve (corresponding to Larive's equation eq. (2.6)) passing through the entire truncated curve and asymptotically connecting with the future uncertainty domain.
   (c) Determine the corresponding key parameters (ε^{∞}, τ_l and τ_c).
   (d) Store the data in the excel file containing the input data (mentioned at the end of section 2.3).

Merlin input data for AAR are generated based on correlated LHS method. In this investigation, there are $n = 56$ simulations and $m = 15$ random variables associated with AAR (table 2.4). Thus,

1. Construct an input matrix $\mathbf{R}_{m\times n}$ defined by m LHS for each of the n RVs.
2. Define a target correlation matrix as $\mathbf{C}_{n\times n}$ where $0 < C_{ij} < 1$ which encapsulates the relationships between variables. It is often a subjective indicator.
3. Compute the sample correlation matrix $\mathbf{T}_{n\times n}$ of $\mathbf{R}_{m\times n}$ by populating each cell of the $n \times n$ matrix with a random number.

4. Perform a Cholesky decomposition of the target correlation matrix $\mathbf{C}_{n\times n} = \mathbf{P}\mathbf{P}^T$.
5. Similarly decompose the sample correlation matrix $\mathbf{T}_{n\times n} = \mathbf{Q}\mathbf{Q}^T$.
6. Determine $\mathbf{S}_{n\times n}$ using either $\mathbf{C} = \mathbf{S}\mathbf{T}\mathbf{S}^T$ or $\mathbf{S} = \mathbf{P}\mathbf{Q}^{-1}$.
7. Generate a $n \times m$ matrix $\mathbf{R}_{s1}$ whose columns represent n independent permutations of an arbitrary set $a(i)$, $i = 1, 2, ..., m$.
8. Convert $\mathbf{R}_{s1}$ to van der Waerden scores, $\mathbf{R}_{s2}$ (Conover, W.J. 1980). The van der Waerden scores are defined as $\Phi^{-1}\left(\frac{i}{m+1}\right)$, $i = 1, 2, ..., m$, where Φ^{-1} is the inverse of the standard normal cumulative distribution function.
9. Re-construct the matrix $\mathbf{R}^*_{n\times n} = \mathbf{R}_{s2}\mathbf{S}^T$. Match up the rank pairing in $\mathbf{R}$ based on $\mathbf{R}^*$.
10. Results are stored as `.mat` (Matlab binary data) file.

Merlin input data for concrete A similar procedure to the previous one is used to generate $n = 56$ simulations and $m = 13$ random variables associated with concrete (table 2.3). Again data re-stored in a separate `.mat` (Matlab binary data) file.

Generate Actual `.inp` files for Merlin analyses. Input sections which are constant are separately stored in ASCII files. For each of the 56 analyses, read a set of (previously randomized) set of data for AAR and concrete, and assemble the actual input file for subsequent run with Merlin.

2.5 OUTPUT DATA; RECODERS LOCATION

Given the reported location of the sensors, fig. 2.5, and the finite element mesh, a program was written to identify the finite element mesh nodes closest to the sensors, table 2.5.

Point of measurement in the finite element mesh are commonly refereed to as "recorders".

Table 2.5. Strain gages location points, and corresponding closest Merlin nodes

		Coord. [inches]			Coord. [meter]			Merlin Closest Nodes			
ID	DOF	x	y	z	x	y	z	Node	x	y	z
S1	3	33	23	20	0.838	0.584	0.508	4526	0.848	0.610	0.508
S2	3	63	23	20	1.600	0.584	0.508	5191	1.643	0.610	0.508
S3	3	43	33	20	1.092	0.838	0.508	4799	1.082	0.838	0.508
S4	3	53	43	10	1.346	1.092	0.254	5070	1.317	1.067	0.254
S5	3	53	43	20	1.346	1.092	0.508	5072	1.317	1.067	0.508
S6	3	53	43	30	1.346	1.092	0.762	5074	1.317	1.067	0.762
S7	3	63	43	20	1.600	1.092	0.508	5275	1.643	1.067	0.508
S8	3	33	53	20	0.838	1.346	0.508	5506	0.848	1.389	0.508
S9	3	53	53	20	1.346	1.346	0.508	5548	1.317	1.389	0.508
S10	3	63	53	10	1.600	1.346	0.254	5581	1.643	1.389	0.254
S11	3	63	53	20	1.600	1.346	0.508	5583	1.643	1.389	0.508
S12	3	63	53	30	1.600	1.346	0.762	5585	1.643	1.389	0.762
S13	1	38	43	12	0.965	1.092	0.305	5042	1.004	1.067	0.254
S14	1	38	43	28	0.965	1.092	0.711	5046	1.004	1.067	0.762

Continued on next page

		Coord. inches			Coord. meter			Merlin Closest Nodes			
id	dof	x	y	z	x	y	z	node	x	y	z
S15	1	48	23	12	1.219	0.584	0.305	4559	1.239	0.610	0.254
S16	1	48	23	28	1.219	0.584	0.711	4563	1.239	0.610	0.762
S17	1	58	53	12	1.473	1.346	0.305	1952	1.473	1.389	0.254
S18	1	58	53	28	1.473	1.346	0.711	1960	1.473	1.389	0.762
S19	2	63	28	12	1.600	0.711	0.305	5203	1.643	0.686	0.254
S20	2	63	28	28	1.600	0.711	0.711	5207	1.643	0.686	0.762
S21	2	33	38	12	0.838	0.965	0.305	4944	0.848	0.991	0.254
S22	2	33	38	28	0.838	0.965	0.711	4948	0.848	0.991	0.762
S23	2	63	48	12	1.600	1.219	0.305	1306	1.643	1.219	0.254
S24	2	63	48	28	1.600	1.219	0.711	1310	1.643	1.219	0.762

Similarly, locations of the demountable mechanical strain gauge (DEMEC) points were correlated with finite element nodes, table 2.6.

Table 2.6. Demec location points, and corresponding closest Merlin nodes

Coord. inches			meter			Merlin Closest Nodes			
x	y	z	x	y	z	node	x	y	z
40	30	40	1.016	0.762	1.016	2719	1.0043	0.7620	1.0160
68	30	40	1.7272	0.762	1.016	457	1.7272	0.7620	1.0160
40	58	40	1.016	1.4732	1.016	277	1.0043	1.4732	1.0160
68	58	40	1.7272	1.4732	1.016	50	1.7272	1.4732	1.0160

Differential displacements between these points (to be measured with a DEMEC), were assigned to elongation recorders shown in table 2.7.

Table 2.7. Numerical gages in Merlin

Numerical gages			
ID	From	To	dof
E1	2719	457	1
E2	2719	277	2
E3	277	50	1
E4	457	50	2

Two vertical displacements were recorded at the center of the panel (top and bottom), table 2.8.

Table 2.8. Coordinates of the vertical displacement recorders (m)

ID	x	y	z
D1-Top	2.5212	2.2672	1.016
D2-Bottom	2.5212	2.2672	0.000

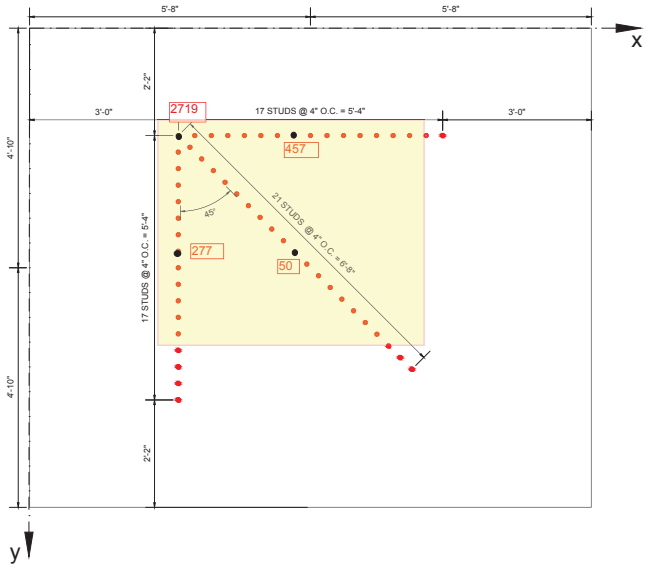

(a) Location of demec points and corresponding FE nodes

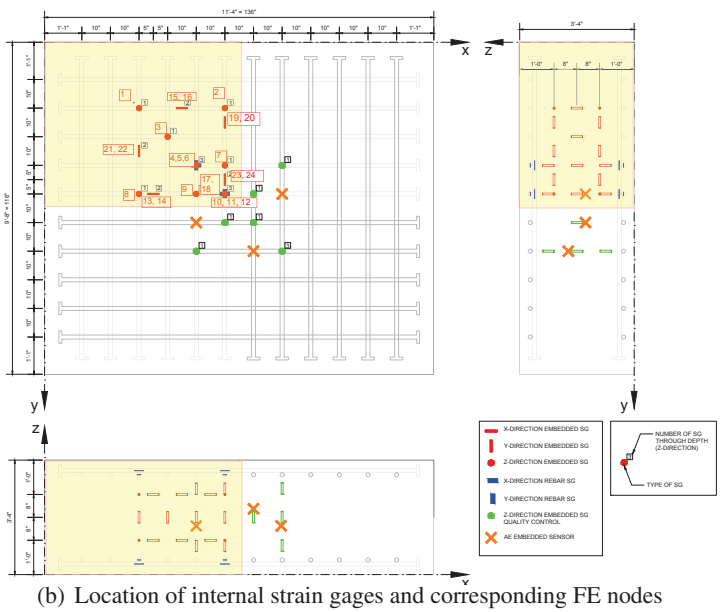

(b) Location of internal strain gages and corresponding FE nodes

Fig. 2.5. Sensors physical and numerical locations

fig. 2.6 shows the correspondence between physical sensors, and numerical recorders for the concrete.

Finally, reinforcement strains and stresses were recorded from the finite element analysis, table 2.9 and are shown in fig. 2.7.

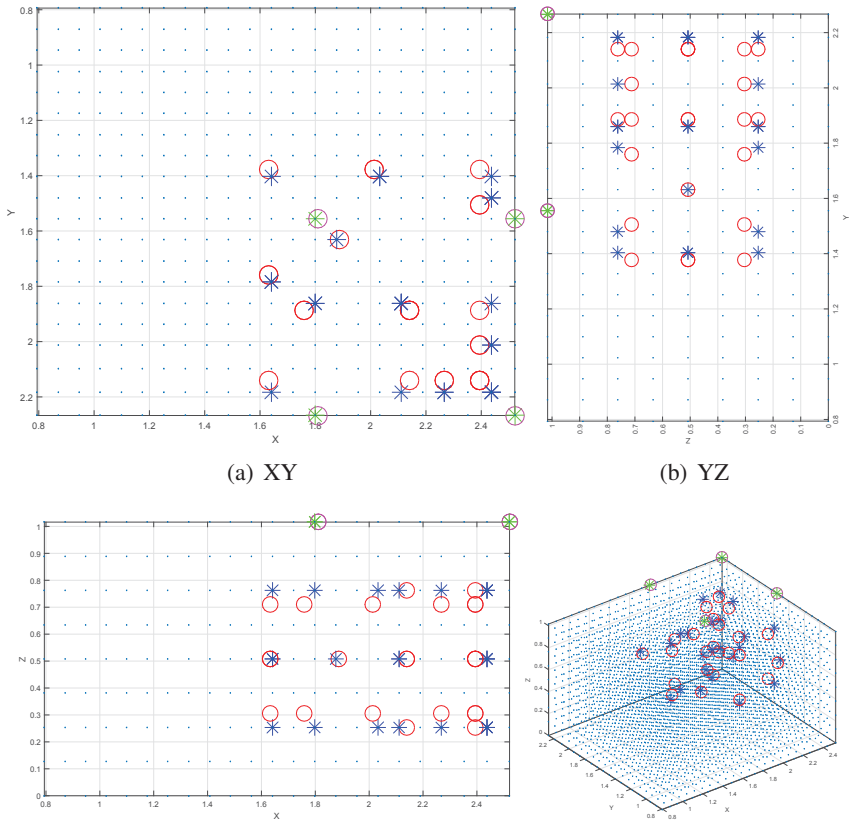

(a) XY (b) YZ

(c) XZ (d) Isometric

Fig. 2.6. Locations of sensors and data point recorders in the finite element mesh

Table 2.9. Location of reinforcement strain gages

ID	x	y	z
R1	1.632	1.378	0.0953
R2	2.14	1.886	0.0953
R3	1.632	1.378	0.9208
R4	2.14	1.886	0.9208
R5	1.632	1.378	0.1334
R6	2.14	1.886	0.1334
R7	1.632	1.378	0.8827
R8	2.14	1.886	0.8827

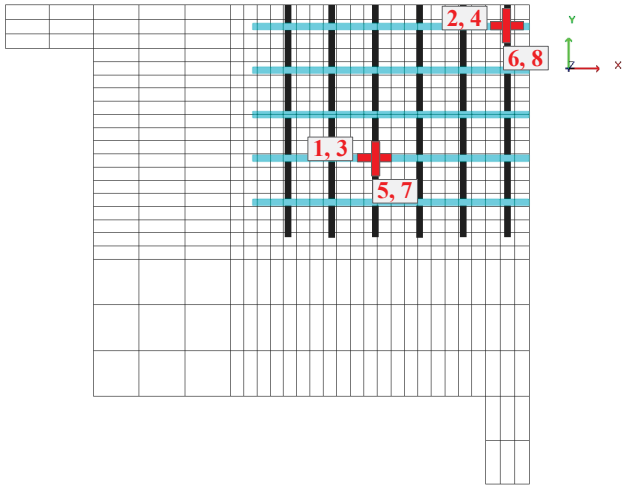

Fig. 2.7. Location of reinforcement strain gages and recorders

2.6 ANALYSIS PROCEDURE

Again, in the spirit of the probabilistic approach 56 analyses were performed. The procedure to generate each input file was explained above. The actual (Matlab based) procedure hinges on a sequence of five program `P1.m`, `P2.m`, `P3.m`, `P4.m` and `P5.m`, fig. 2.8.

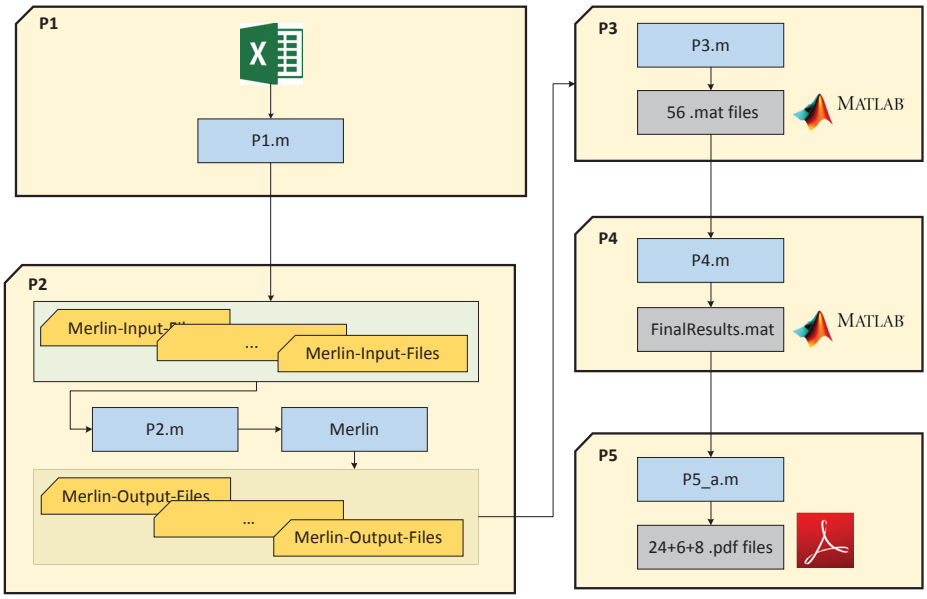

Fig. 2.8. File generation algorithm

P1 starts with the mesh generator Kumo to generate a generic finite element mesh for a given geometry, depth and boundary condition. The file is then split in three parts. The first and last one are retained as they are valid to all analyses, the middle one is discarded. Then the program `P1.m` reads those two files and within its own internal loop inserts the missing part (concrete and AAR parameters).

P2 will in turn run all the 56 analyses with Merlin (by far the most computationally intensive task).

P3 Will read the Merlin output files (ASCII) and save the relevant results in binary form as individual `.mat` files.

P4 consolidates all the 56 individual `.mat` files into a single one.

P5 does perform the final post-processing and plots the results as `.pdf` files to be then inserted in the LaTeXreport. For each locater, all results will be plotted along with their mean and 16 and 84 percentile ranges which correspond to minus and plus one standard deviation, fig. 2.9.

2.7 GENERATED DATA

Implementation of the above described procedure resulted in the generation of 56 input data files. The variables associated with each one of them is tabulated in table 2.10. The variables associated with he

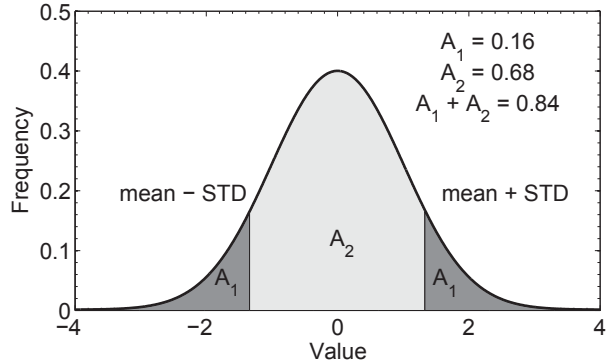

Fig. 2.9. Standard deviation *vs.* percentile definition for normal distribution

concrete model are clearly separated from those associated with the AAR uncertainty. Note that analyses # 16, 40 and 42 failed to converge due to numerical instability.

Table 2.10. Generated random variables based on LHS

	Concrete					AAR								
RV_{ID}	4	6	7	8	11	2	3	4	5	6	7	8	14	15
	E	f_t'	G_F	f_c'	e	ε^{∞}	τ_c	tau_l	U_c	U_l	RRF	FoT	β_E	β_{ft}
1	25,873	2.90	1.064E-04	-23.3	0.56	0.0050	82.0	329.4	5,096	10,117	0.60	0.50	0.53	0.67
2	22,076	2.65	1.113E-04	-21.4	0.67	0.0080	87.0	372.7	5,453	8,516	0.43	0.47	0.59	0.51
3	28,880	2.19	9.030E-05	-23.4	0.63	0.0055	81.5	325.7	5,350	8,700	0.42	0.46	0.69	0.59
4	27,844	2.81	5.861E-05	-24.3	0.64	0.0075	84.0	344.8	5,391	10,268	0.40	0.45	0.66	0.56
5	25,705	3.16	1.003E-04	-21.7	0.55	0.0065	83.3	339.5	5,460	9,597	0.51	0.62	0.69	0.63
6	23,125	2.59	1.247E-04	-25.1	0.61	0.0050	73.1	277.5	4,867	9,602	0.59	0.61	0.61	0.64
7	23,420	2.86	1.002E-04	-19.6	0.67	0.0045	76.4	293.3	5,701	9,998	0.46	0.43	0.57	0.69
8	30,176	2.82	1.157E-04	-20.5	0.68	0.0045	74.6	283.4	4,989	9,093	0.46	0.64	0.52	0.48
9	20,230	2.56	1.241E-04	-22.5	0.65	0.0065	90.4	410.8	5,126	10,335	0.56	0.44	0.62	0.52
10	21,222	3.03	7.795E-05	-24.6	0.77	0.0040	72.3	271.8	5,574	8,491	0.40	0.49	0.60	0.59
11	29,445	2.48	1.174E-04	-23.9	0.51	0.0040	68.5	254.5	5,567	9,887	0.41	0.36	0.53	0.66
12	28,528	2.59	7.854E-05	-22.2	0.53	0.0055	78.7	305.8	5,937	8,539	0.44	0.38	0.54	0.50
13	26,901	3.09	1.019E-04	-22.7	0.60	0.0070	80.9	321.7	5,027	9,439	0.39	0.46	0.49	0.71
14	21,588	2.35	7.464E-05	-18.7	0.70	0.0050	76.9	296.4	5,829	9,641	0.45	0.57	0.60	0.57
15	25,986	3.07	9.573E-05	-16.4	0.56	0.0060	79.6	312.9	5,136	9,108	0.65	0.40	0.65	0.62
16	24,093	2.54	6.413E-05	-18.0	0.67	0.0065	85.7	359.8	5,213	8,848	0.50	0.59	0.67	0.70
17	24,683	2.77	9.326E-05	-22.3	0.58	0.0045	81.8	326.8	4,976	10,215	0.37	0.56	0.63	0.63
18	19,981	2.75	1.121E-04	-19.8	0.64	0.0060	82.8	335.7	5,200	10,274	0.44	0.49	0.55	0.51
19	26,178	2.51	6.595E-05	-17.8	0.60	0.0040	71.6	268.2	5,614	9,517	0.36	0.47	0.65	0.57
20	24,561	2.74	8.244E-05	-20.5	0.77	0.0080	86.2	363.6	5,606	8,686	0.38	0.44	0.48	0.58
21	23,741	2.62	9.900E-05	-21.5	0.58	0.0040	83.2	339.0	5,542	10,010	0.52	0.49	0.56	0.53
22	25,147	2.39	9.800E-05	-19.2	0.71	0.0045	72.0	270.2	4,893	9,493	0.55	0.53	0.51	0.50
23	23,138	2.55	1.197E-04	-17.4	0.62	0.0045	85.1	355.9	5,532	8,654	0.63	0.58	0.65	0.69
24	21,710	2.71	8.957E-05	-21.2	0.75	0.0045	74.5	283.2	4,930	9,184	0.58	0.63	0.61	0.65
25	22,729	2.64	8.201E-05	-20.8	0.54	0.0075	81.2	324.0	5,076	8,809	0.34	0.43	0.68	0.52
26	22,388	2.31	8.701E-05	-24.1	0.62	0.0050	86.0	362.0	5,400	9,212	0.52	0.51	0.71	0.68
27	24,971	2.76	8.557E-05	-17.1	0.73	0.0055	77.3	298.3	5,229	8,994	0.61	0.58	0.59	0.67
28	25,509	2.73	8.797E-05	-21.3	0.56	0.0055	80.7	319.4	5,687	9,429	0.51	0.54	0.63	0.54
29	25,614	2.94	8.411E-05	-22.1	0.66	0.0060	86.7	369.5	5,432	8,619	0.57	0.50	0.51	0.55

Continued on next page

	Concrete					AAR								
RVid	4	6	7	8	11	2	3	4	5	6	7	8	14	15
	E	f'_t	G_F	f'_c	e	ε^{∞}	τ_c	tau_l	U_c	U_l	RRF	FoT	β_E	β_{ft}
30	24,834	2.82	6.079E-05	-18.3	0.57	0.0080	92.0	433.0	5,665	9,945	0.46	0.68	0.63	0.72
31	26,701	2.46	1.221E-04	-18.5	0.55	0.0090	88.9	392.6	5,895	8,581	0.55	0.42	0.51	0.52
32	28,190	2.72	7.596E-05	-23.0	0.66	0.0085	87.2	374.6	5,285	9,540	0.63	0.54	0.57	0.67
33	24,166	2.71	1.194E-04	-19.9	0.72	0.0055	82.4	329.6	5,505	9,335	0.54	0.51	0.54	0.66
34	19,249	3.00	7.055E-05	-17.9	0.86	0.0050	79.1	308.9	5,366	8,783	0.66	0.37	0.62	0.69
35	25,182	2.64	8.012E-05	-21.8	0.68	0.0070	83.8	345.4	5,172	10,170	0.43	0.53	0.68	0.61
36	24,443	2.57	1.053E-04	-19.4	0.58	0.0040	70.6	263.6	5,859	9,749	0.53	0.48	0.71	0.60
37	22,915	2.63	1.138E-04	-16.9	0.65	0.0065	87.7	379.9	5,306	9,308	0.49	0.39	0.69	0.71
38	20,518	2.90	9.141E-05	-20.1	0.61	0.0050	75.4	289.5	5,783	10,194	0.56	0.59	0.58	0.65
39	26,248	2.61	1.029E-04	-19.5	0.58	0.0065	82.5	332.1	5,000	8,881	0.45	0.57	0.64	0.49
40	30,607	2.38	1.152E-04	-15.8	0.70	0.0055	83.5	342.3	5,733	9,728	0.47	0.51	0.66	0.64
41	28,001	2.45	8.478E-05	-19.0	0.52	0.0070	86.5	369.6	4,904	8,731	0.62	0.55	0.68	0.50
42	22,170	2.69	7.431E-05	-17.7	0.72	0.0070	82.2	330.7	5,340	9,149	0.50	0.48	0.57	0.53
43	23,956	2.92	1.297E-04	-22.8	0.53	0.0085	86.2	365.7	5,873	8,913	0.42	0.60	0.55	0.56
44	27,461	2.67	1.096E-04	-21.0	0.60	0.0060	84.0	344.7	5,063	10,097	0.49	0.32	0.61	0.57
45	25,356	2.84	1.043E-04	-19.2	0.54	0.0050	71.3	267.3	5,640	9,062	0.48	0.40	0.53	0.49
46	27,666	2.79	1.278E-04	-18.9	0.65	0.0075	82.3	331.4	5,749	8,962	0.59	0.52	0.56	0.60
47	23,448	2.69	1.072E-04	-16.1	0.61	0.0055	81.0	323.1	5,907	10,043	0.49	0.41	0.49	0.62
48	27,298	2.42	9.681E-05	-20.6	0.69	0.0060	84.6	349.6	4,941	9,374	0.54	0.55	0.70	0.68
49	27,119	2.95	1.082E-04	-23.6	0.64	0.0065	78.7	307.3	5,043	9,695	0.48	0.52	0.59	0.55
50	29,241	2.98	1.306E-04	-21.9	0.63	0.0070	78.9	308.8	5,151	9,236	0.51	0.67	0.51	0.55
51	24,353	2.67	6.212E-05	-20.2	0.62	0.0045	79.5	314.5	5,726	9,913	0.59	0.43	0.50	0.62
52	23,649	2.52	6.981E-05	-20.4	0.54	0.0060	79.7	313.6	5,255	9,278	0.47	0.65	0.67	0.63
53	26,625	2.88	9.439E-05	-19.7	0.57	0.0040	74.2	281.6	5,491	9,769	0.37	0.32	0.49	0.54
54	26,385	2.49	6.861E-05	-16.7	0.52	0.0060	81.1	323.7	5,275	9,030	0.53	0.35	0.56	0.61
55	22,568	2.80	7.196E-05	-18.4	0.59	0.0040	77.0	297.1	5,811	9,855	0.57	0.45	0.70	0.70
56	21,094	2.86	9.199E-05	-21.0	0.59	0.0075	85.4	357.5	5,801	9,819	0.53	0.55	0.72	0.60

Chapter 3

Result

Procedures outlined in section 2.6 was implemented and executed. Hence this chapter will present all results. First, indicative plots associated with one randomly selected analysis are presented and they will provide simple visual and numerical checks. Next, results associated with the probabilistic approach are presented in a way to facilitate future comparison between predicted and observed values.

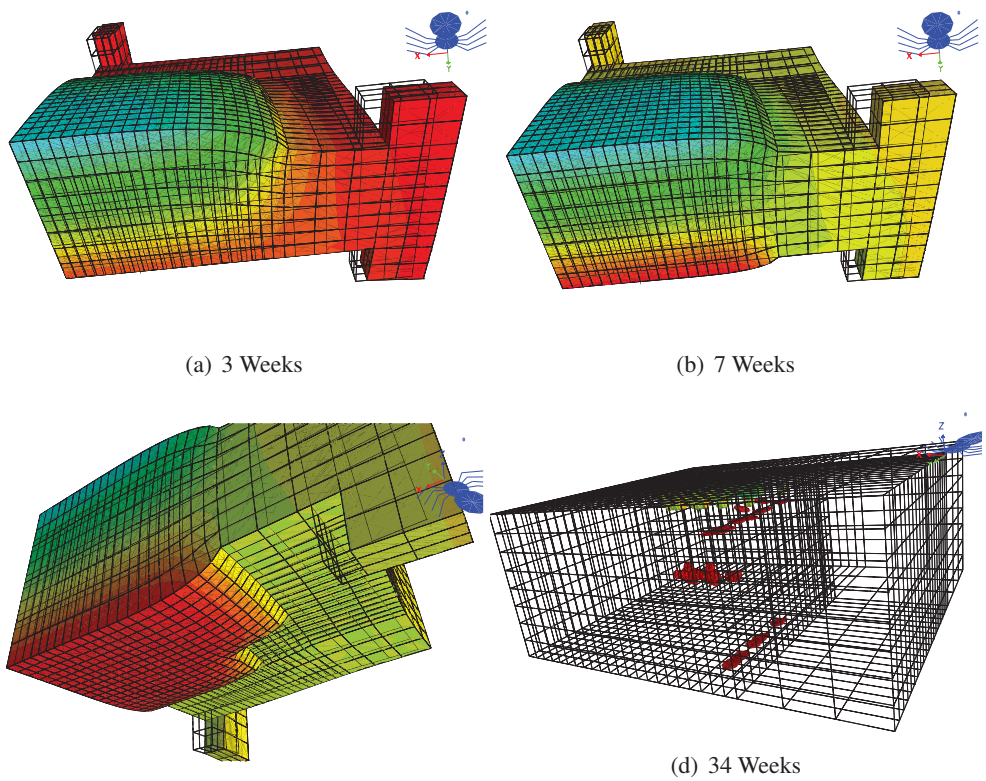

(a) 3 Weeks

(b) 7 Weeks

(c) 7 Weeks

(d) 34 Weeks

Fig. 3.1. Selected views of deformed shapes; contour lines correspond to vertical displacement and crack pattern

3.1 DETERMINISTIC RESULTS

To better grasp response of the specimen, analysis # 3 (table 2.10) was randomly selected to display selective results. fig. 3.1(a) is the initial deformed mesh (with contour plot on z direction displacement) after three weeks, and before the bottom support was removed. By the seventh week, the support was removed and fig. 3.1(b) shows the deformation on both sides of the slab (with the top deformation clearly larger than the one at the bottom). Moreover, this figure shows that the AAR expansion pushes the steel cage outwards and there are some in-plane deformations in steel cage. A bottom view at seven week confirms the restraining effect of the bottom corner support, fig. 3.1(c). Finally, fig. 3.1(d) shows that despite the large expansion at 34 weeks, internal cracking is minimal and localized in vicinity of the steel cage. It should be noted that this may be a parasitic result of the assumption of full contact between concrete and cage. Should some vertical slip allowed, those cracks may be reduced.

On the other hand, the time history of the center top node was tracked. It is shown that the lateral (x and y) confinements induce large internal corresponding (compressive) stresses, as a result of which the corresponding AAR expansion is largely reduced. This is clearly not the case in the z direction and there is a slight tensile stress at the concrete free surface in the vertical direction.

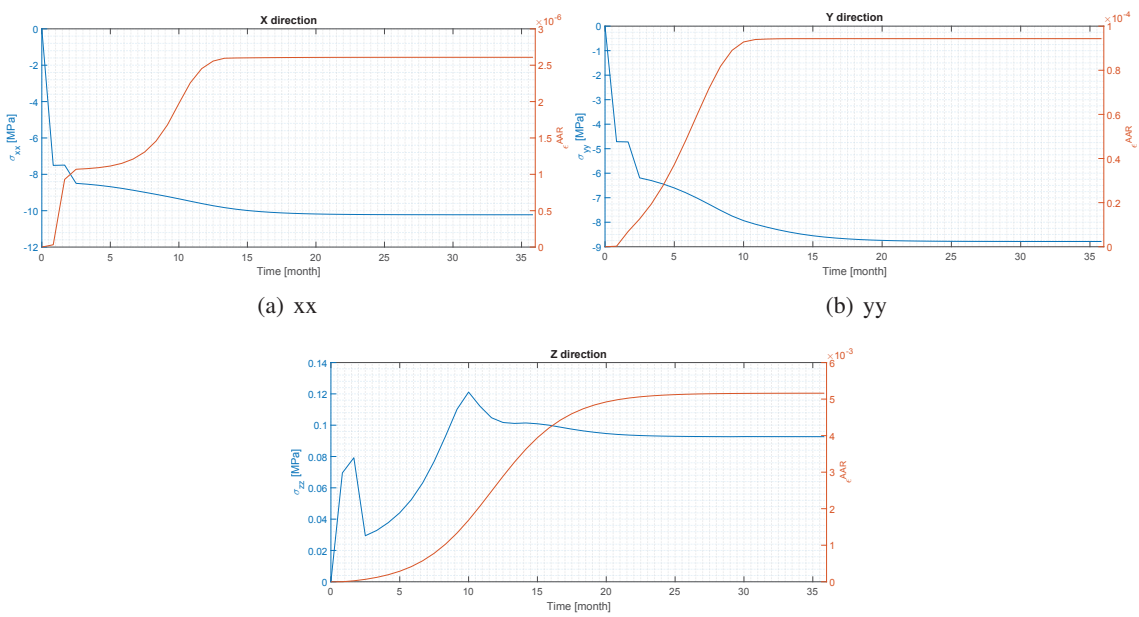

(a) xx (b) yy

(c) zz

Fig. 3.2. Stresses and AAR strains at the top center node

3.2 PROBABILISTIC BASED PREDICTIONS

Again, following the procedure outlined in section 2.6, results of the 56 analyses were compiled in a single `.mat` (Matlab) binary file for plotting. It should be noted that only three analyses failed to converge due to numerical instability resulting from unfavorable combination of the input parameters.

3.2.1 CONCRETE STRAINS AND STRESS HISTOGRAMS

Concrete internal strains and stresses are first reported for each of the 24 sensors and 53 analyses. In all plots the 50, 84, 16 % fractiles are shown. The shaded area correspond to 16-84% fractiles that is mean ± one standard deviation, fig. 2.9. there following observations can be made:

z direction stress/strain fig. 3.3 to fig. 3.14:

1. The final mean strain (50% percentile) is practically the same for all sensors (0.003) with only about 10% variation.
2. Some strain histograms are smoother than others.
3. Variation is non-negligible within the ± one standard deviation domain. In some cases there is a sudden strain discontinuity (and a corresponding one for the stress).
4. The stress histograms vary substantially in the 50% percentile in the near end. Stress varied depending on the location of the recorder (bottom, inside, or top of the concrete). These values vary from -1.0 to +0.6 MPa at the end of expansion for the median curve.
5. Since the bottom support is removed after 4 weeks (28 days), this is clearly captured in the stress histograms.

x direction stress/strain fig. 3.15 to fig. 3.20:

1. In all cases, the strain time history starts as a positive value (tension) proceeds along the classical sigmoidal shape and ends with a negative value (compression). All median curves are in the 0.0007 to -0.0005 range, however, this range varies with recorder location.
2. In all cases, it takes about 12 months for the strain to shift from positive to negative values.
3. All six stress time histories are negative (compressive) values ranging from -6 to -8 MPa at the end of expansion for the median curve[1].
4. There is more uncertainty in stress than in strain.

y direction stress/strain fig. 3.21 to fig. 3.26:

- In all cases, the strain time history first increases for 6-8 months, and then slowly decrease to a very small strain at the end of expansion.
- In all cases, the stress has negative value (in compression) similar to the x direction.

[1]Recall that the strain is composed of two parts, $\varepsilon = \sigma/E + \varepsilon^{AAR}$ for 1D linear elastic systems, hence stress and strains may have opposite signs

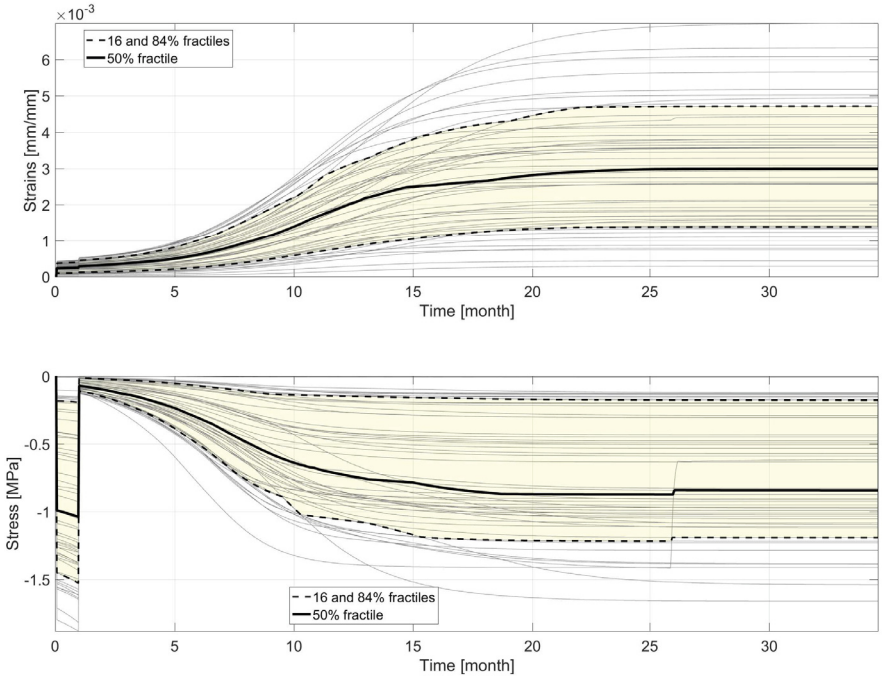

Fig. 3.3. Stress & Strains at Locator # 1, DOF = 3, Coordinates (m)<0.8382, 0.5842, 0.508>

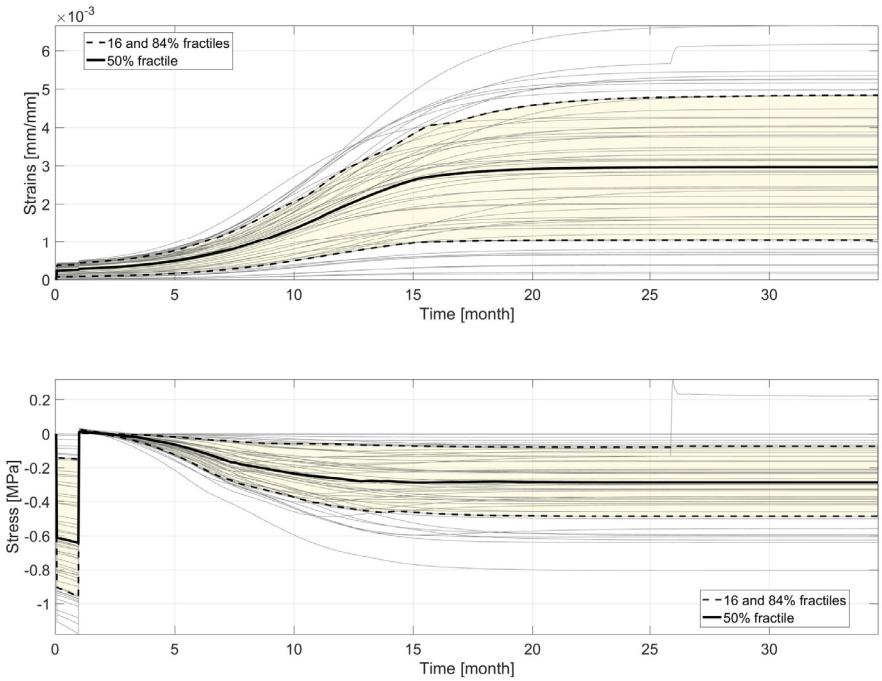

Fig. 3.4. Stress & Strains at Locator # 2, DOF = 3, Coordinates (m)<1.6002, 0.5842, 0.508>

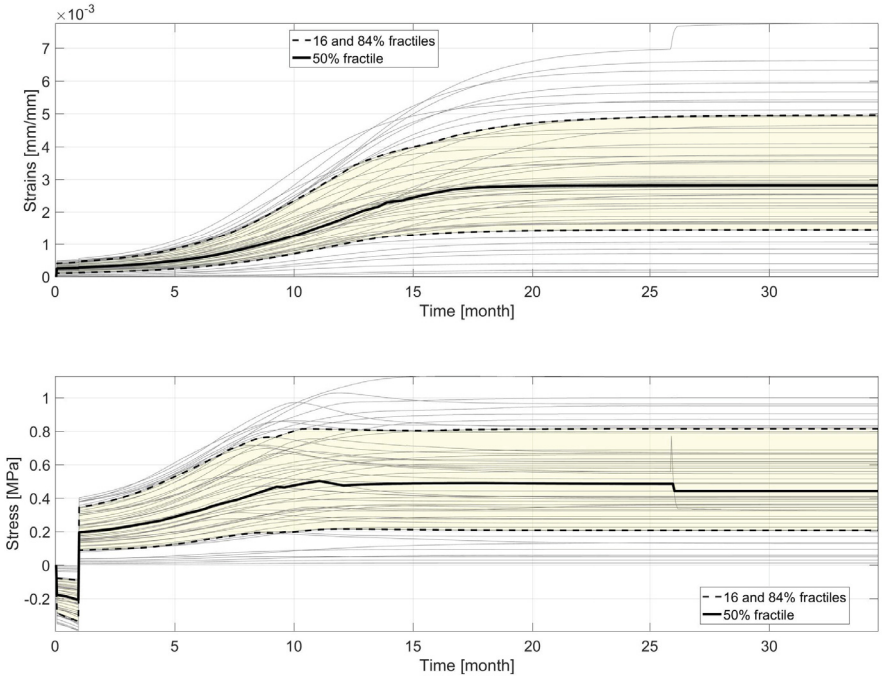

Fig. 3.5. Stress & Strains at Locator # 3, DOF = 3, Coordinates (m)<1.0922, 0.8382, 0.508>

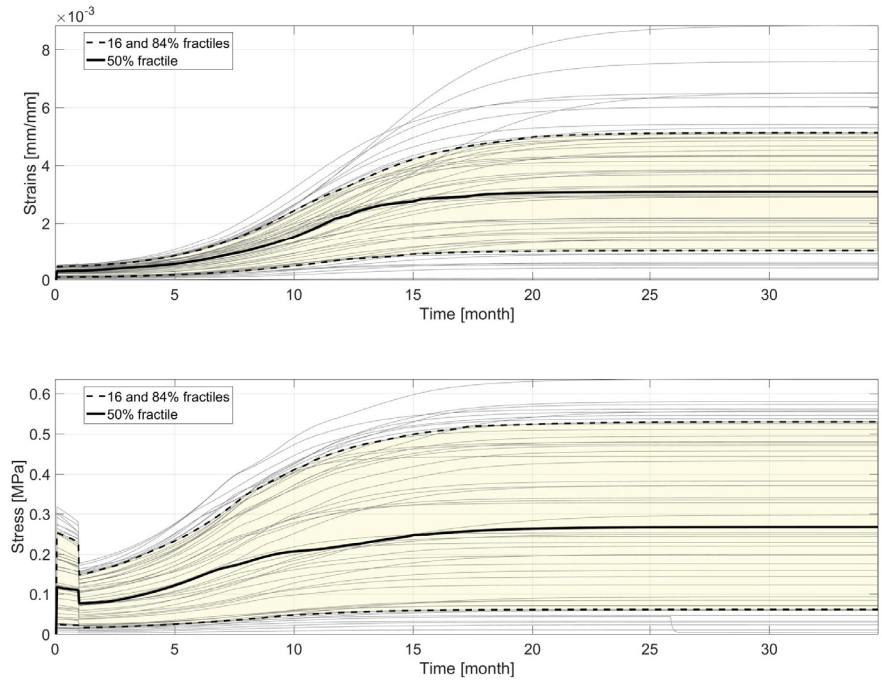

Fig. 3.6. Stress & Strains at Locator # 4, DOF = 3, Coordinates (m)<1.3462, 1.0922, 0.254>

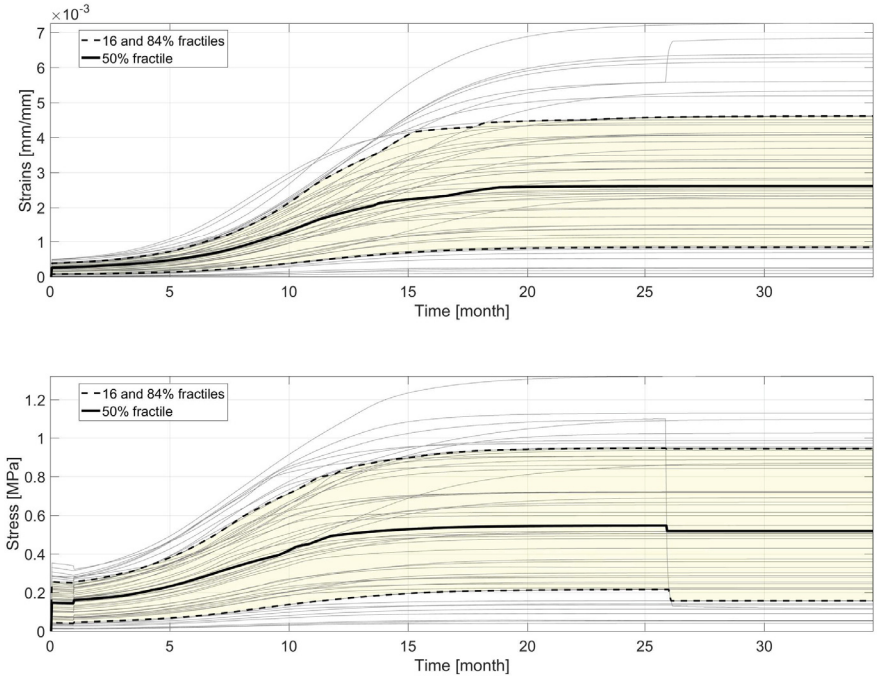

Fig. 3.7. Stress & Strains at Locator # 5, DOF = 3, Coordinates (m)<1.3462, 1.0922, 0.508>

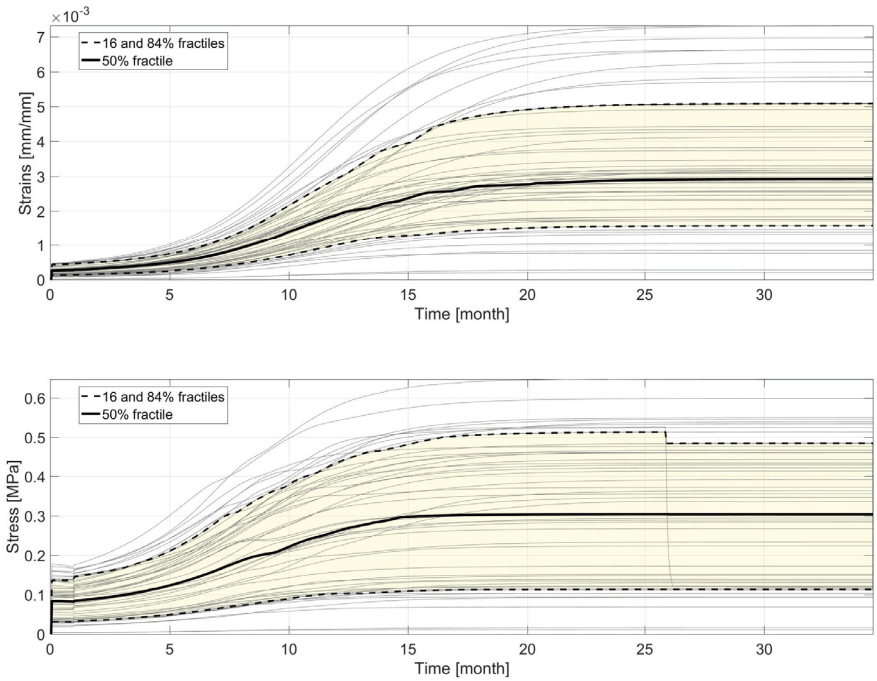

Fig. 3.8. Stress & Strains at Locator # 6, DOF = 3, Coordinates (m)<1.3462, 1.0922, 0.762>

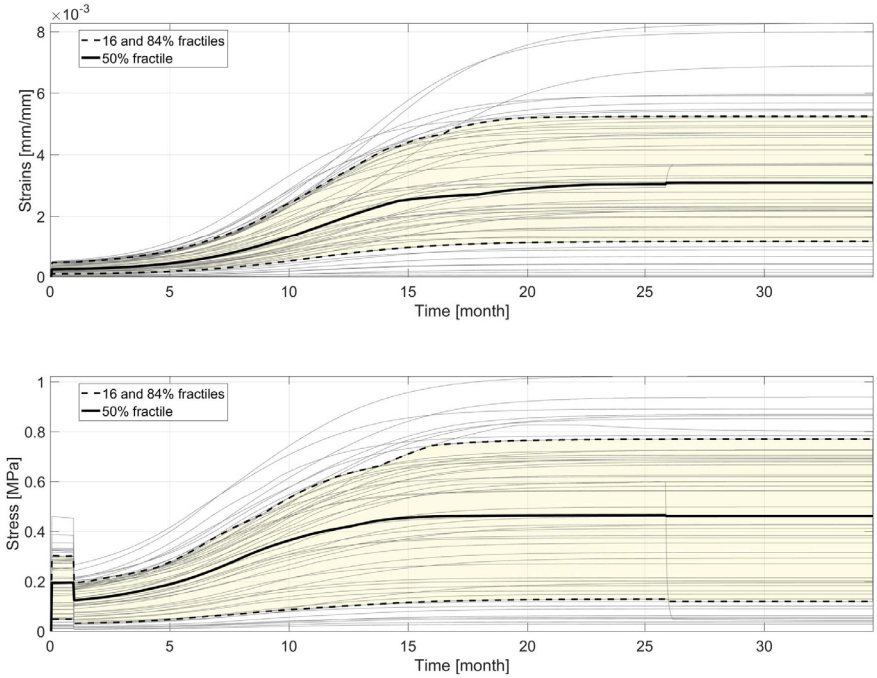

Fig. 3.9. Stress & Strains at Locator # 7, DOF = 3, Coordinates (m)<1.6002, 1.0922, 0.508>

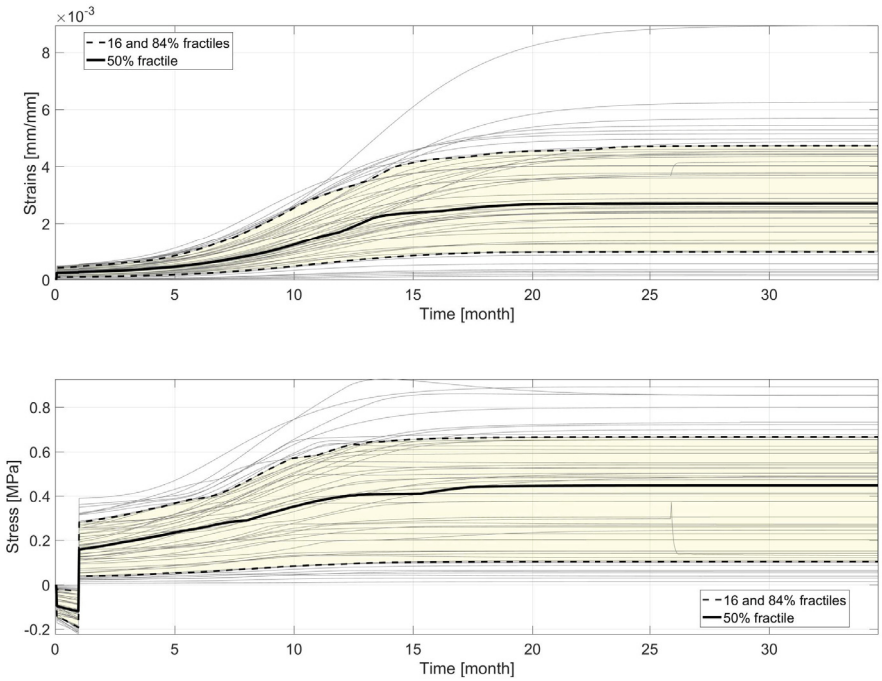

Fig. 3.10. Stress & Strains at Locator # 8, DOF = 3, Coordinates (m)<0.8382, 1.3462, 0.508>

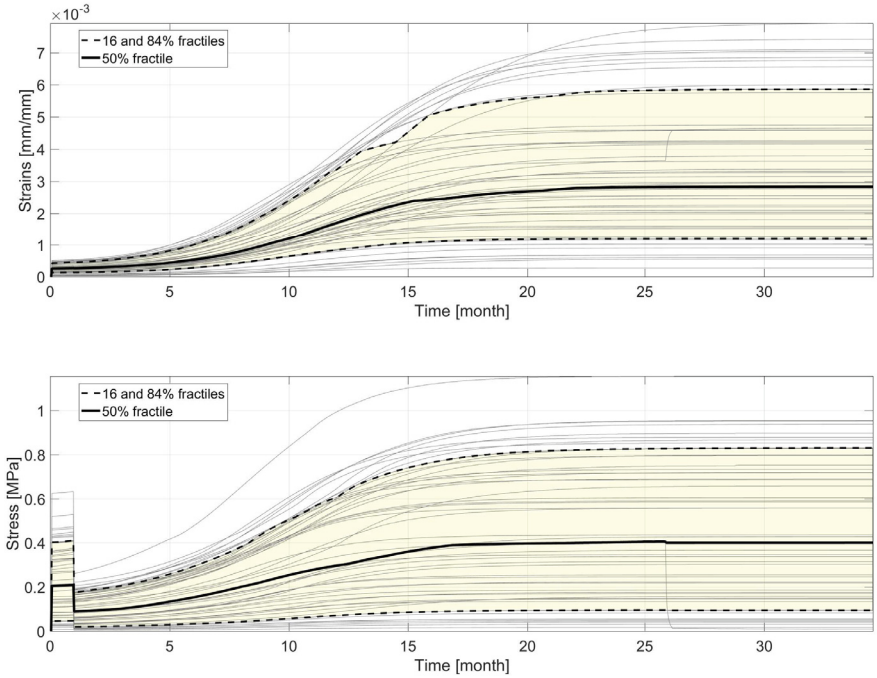

Fig. 3.11. Stress & Strains at Locator # 9, DOF = 3, Coordinates (m)<1.3462, 1.3462, 0.508>

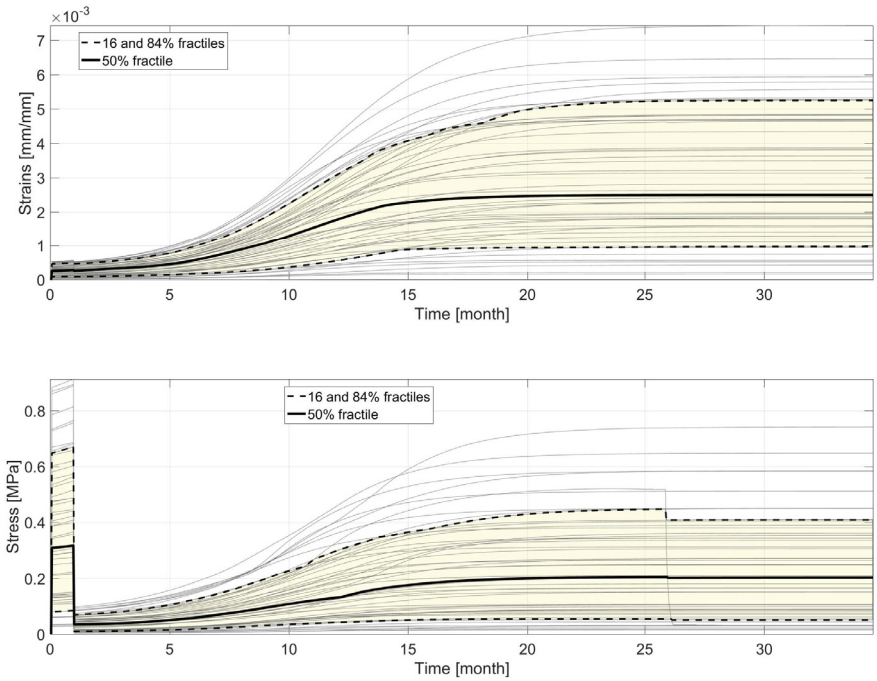

Fig. 3.12. Stress & Strains at Locator # 10, DOF = 3, Coordinates (m)<1.6002, 1.3462, 0.254>

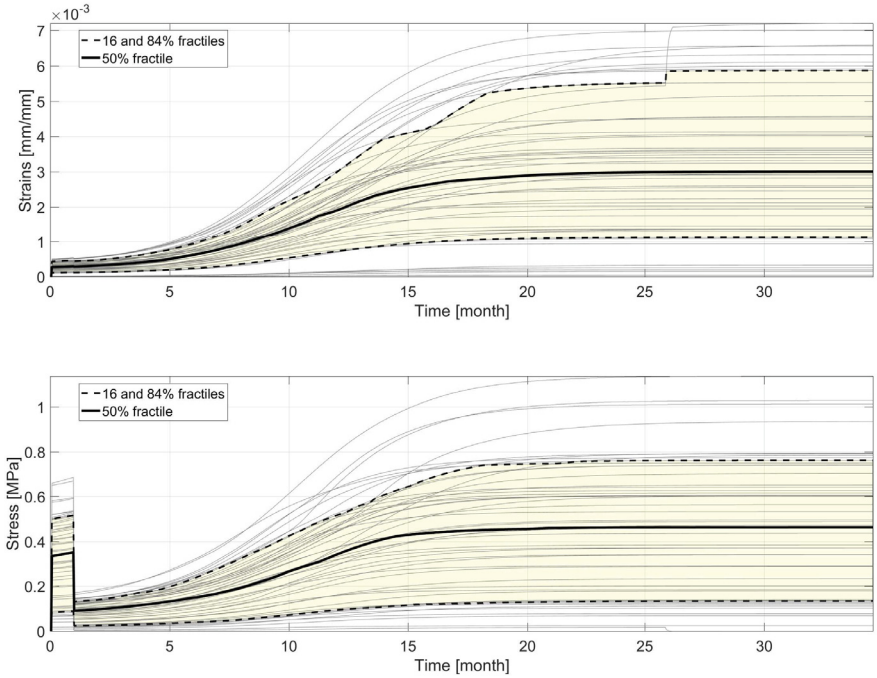

Fig. 3.13. Stress & Strains at Locator # 11, DOF = 3, Coordinates (m)<1.6002, 1.3462, 0.508>

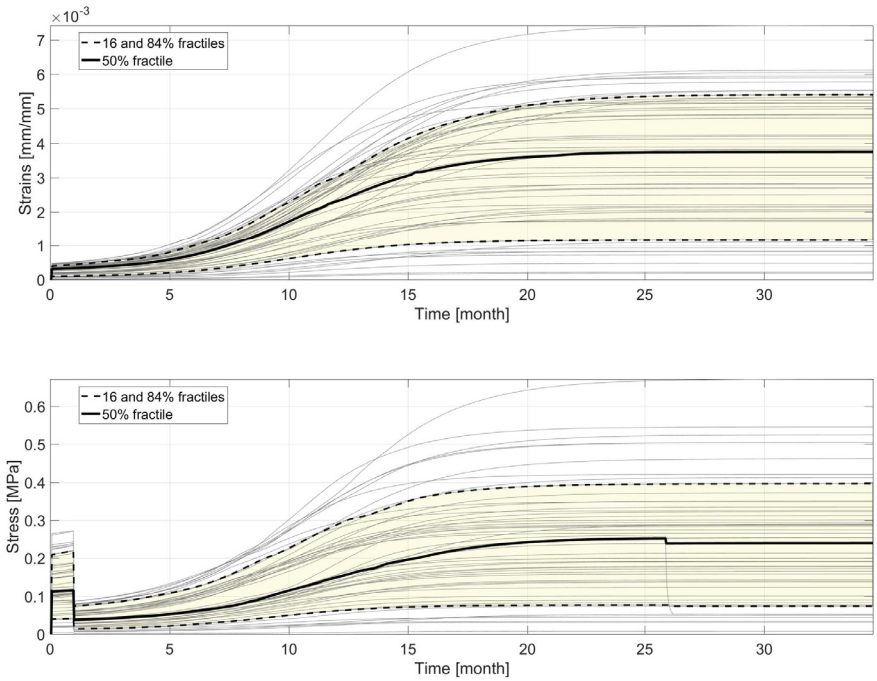

Fig. 3.14. Stress & Strains at Locator # 12, DOF = 3, Coordinates (m)<1.6002, 1.3462, 0.762>

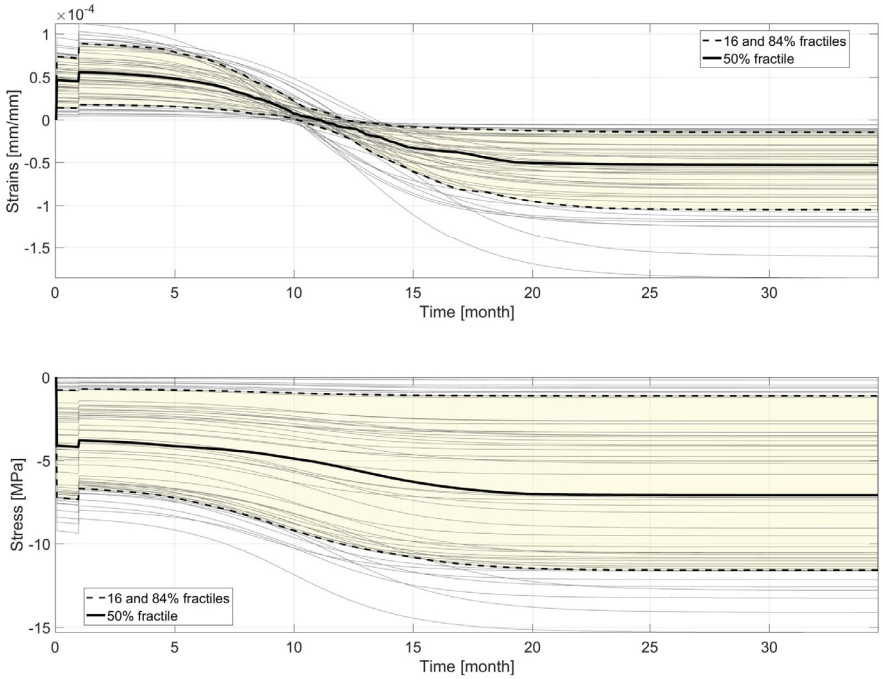

Fig. 3.15. Stress & Strains at Locator # 13, DOF = 1, Coordinates (m)<0.9652, 1.0922, 0.3048>

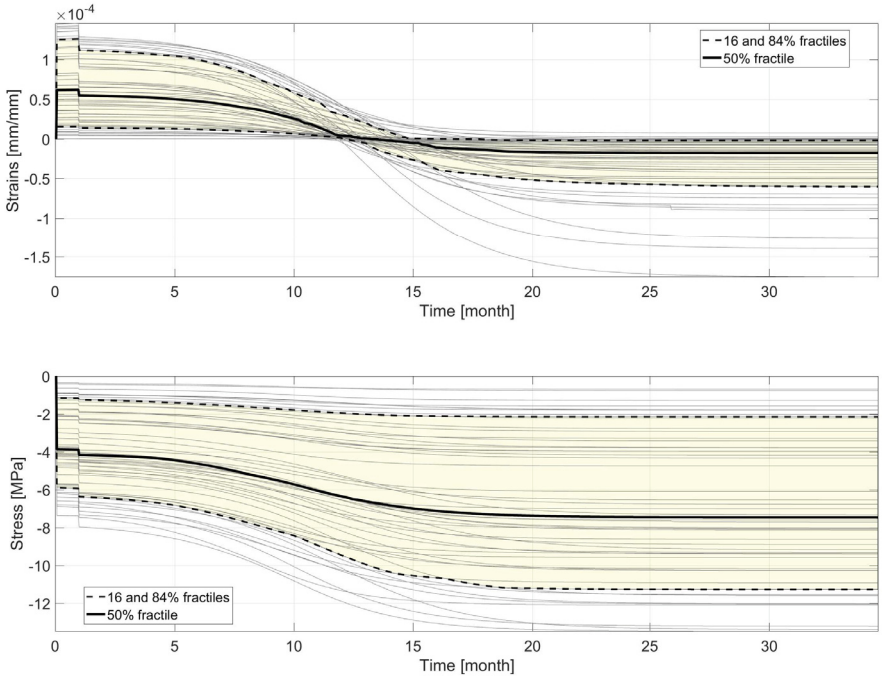

Fig. 3.16. Stress & Strains at Locator # 14, DOF = 1, Coordinates (m)<0.9652, 1.0922, 0.7112>

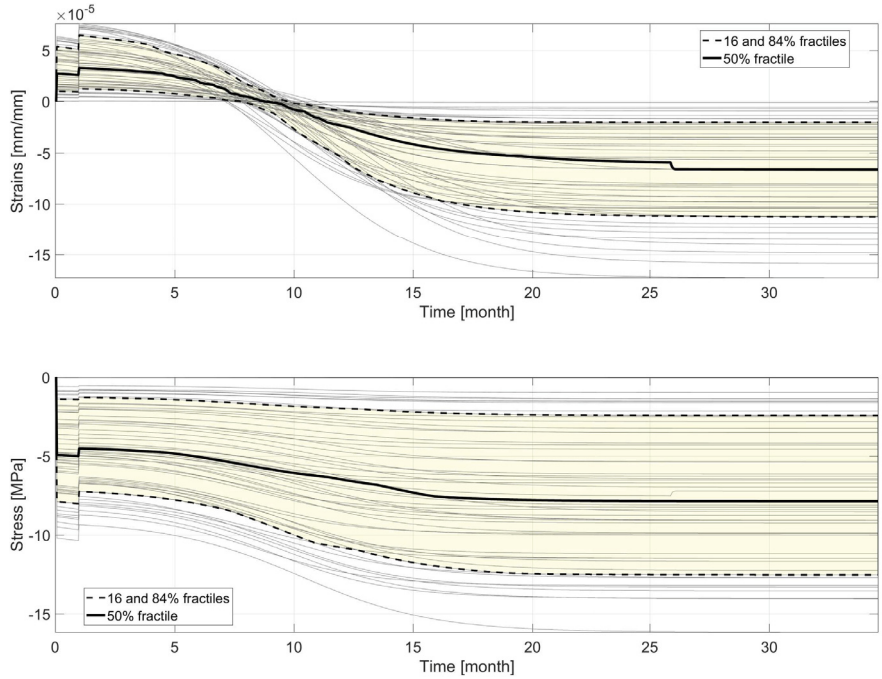

Fig. 3.17. Stress & Strains at Locator # 15, DOF = 1, Coordinates (m)<1.2192, 0.5842, 0.3048>

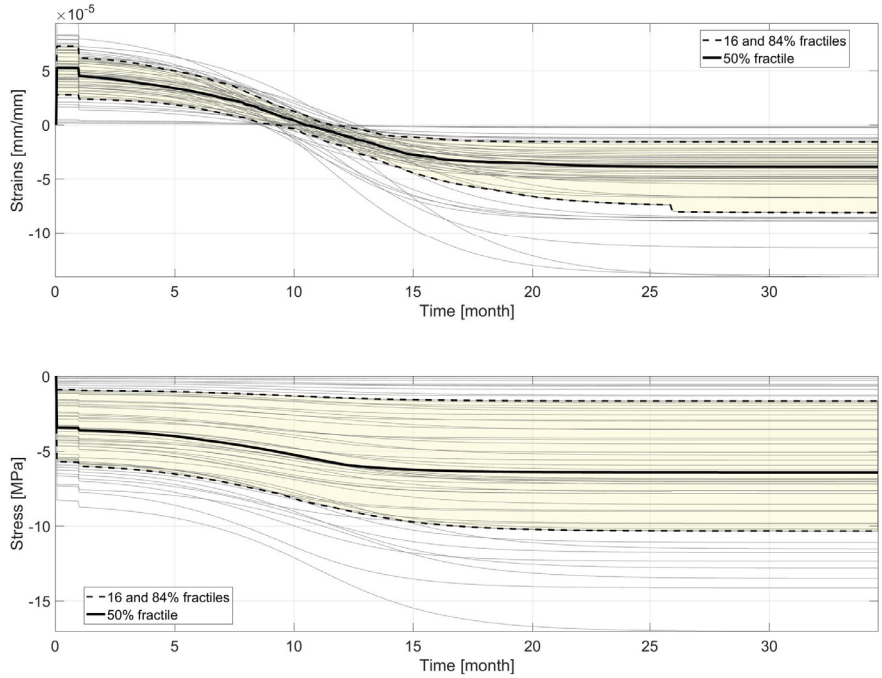

Fig. 3.18. Stress & Strains at Locator # 16, DOF = 1, Coordinates (m)<1.2192, 0.5842, 0.7112>

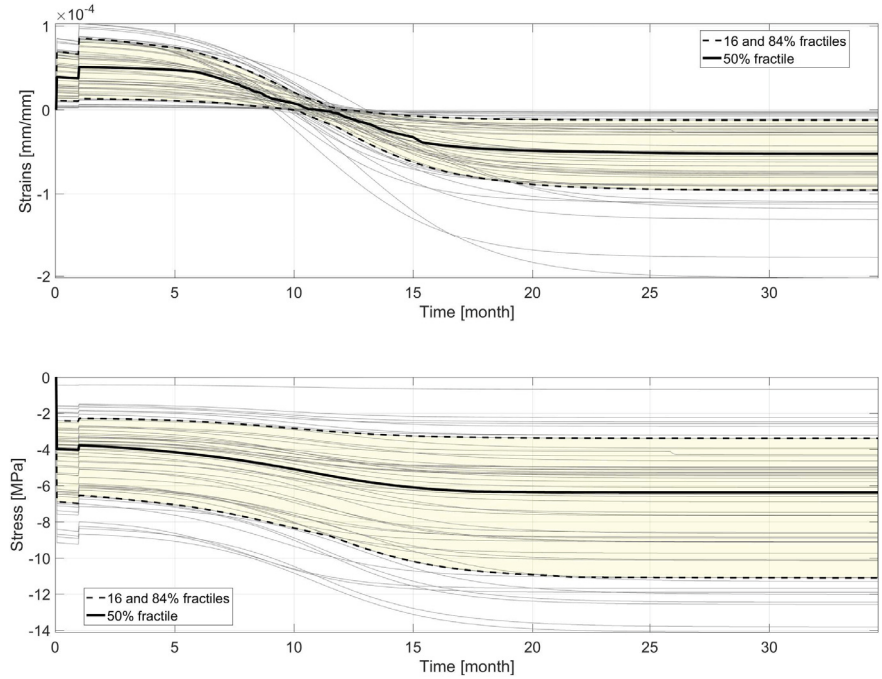

Fig. 3.19. Stress & Strains at Locator # 17, DOF = 1, Coordinates (m)<1.4732, 1.3462, 0.3048>

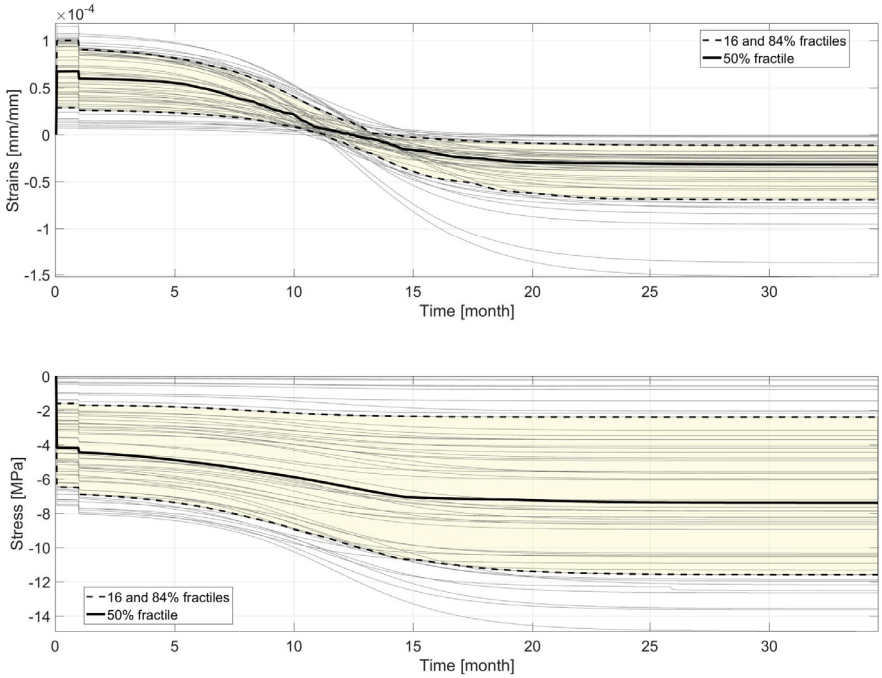

Fig. 3.20. Stress & Strains at Locator # 18, DOF = 1, Coordinates (m)<1.4732, 1.3462, 0.7112>

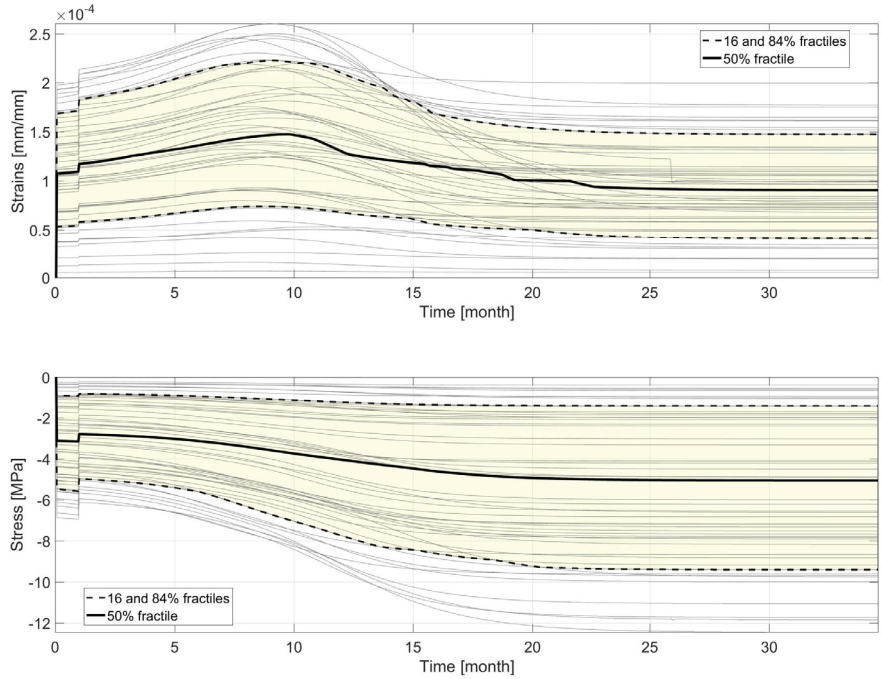

Fig. 3.21. Stress & Strains at Locator # 19, DOF = 2, Coordinates (m)<1.6002, 0.7112, 0.3048>

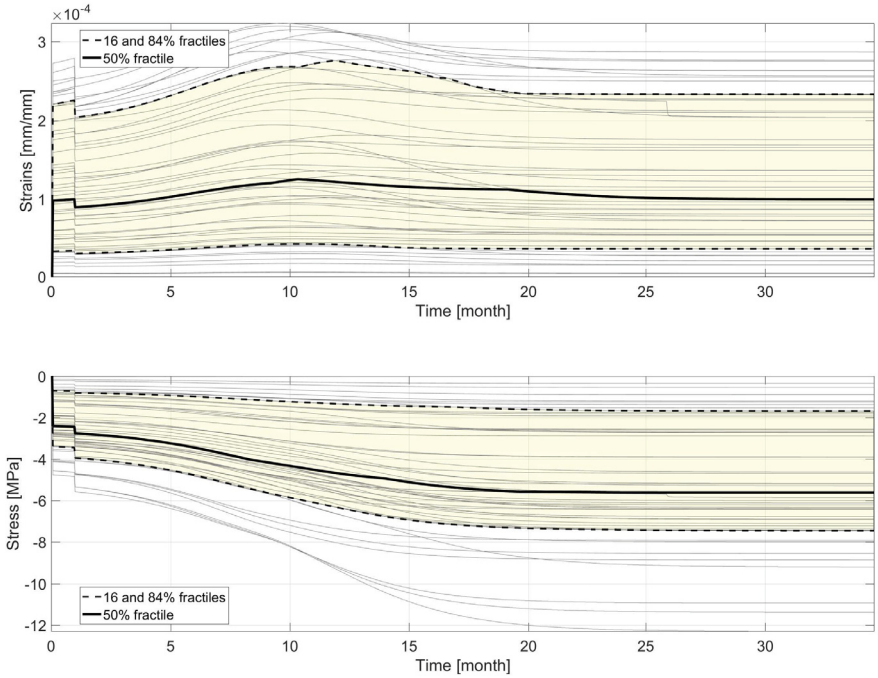

Fig. 3.22. Stress & Strains at Locator # 20, DOF = 2, Coordinates (m)<1.6002, 0.7112, 0.7112>

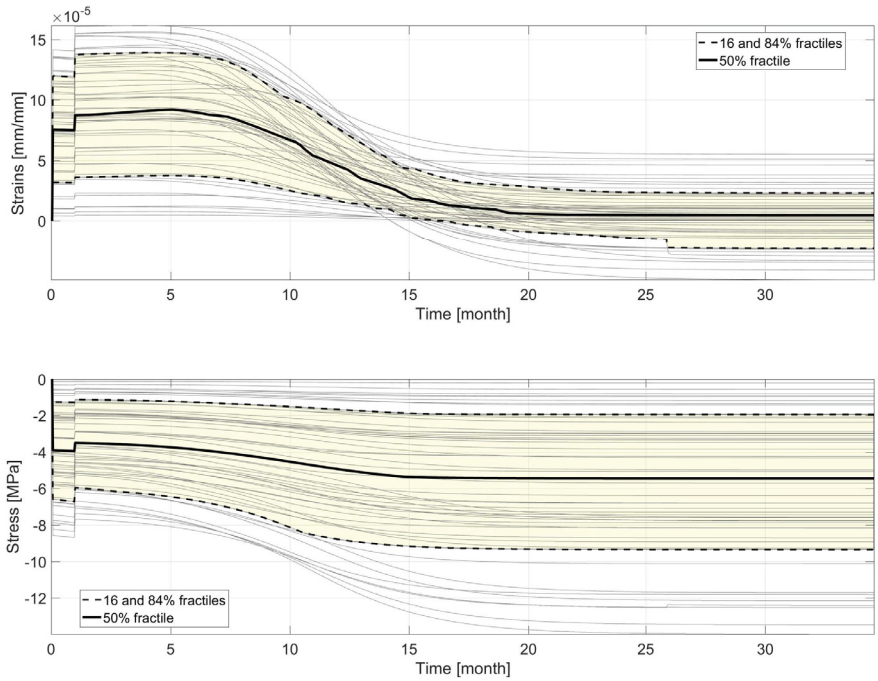

Fig. 3.23. Stress & Strains at Locator # 21, DOF = 2, Coordinates (m)<0.8382, 0.9652, 0.3048>

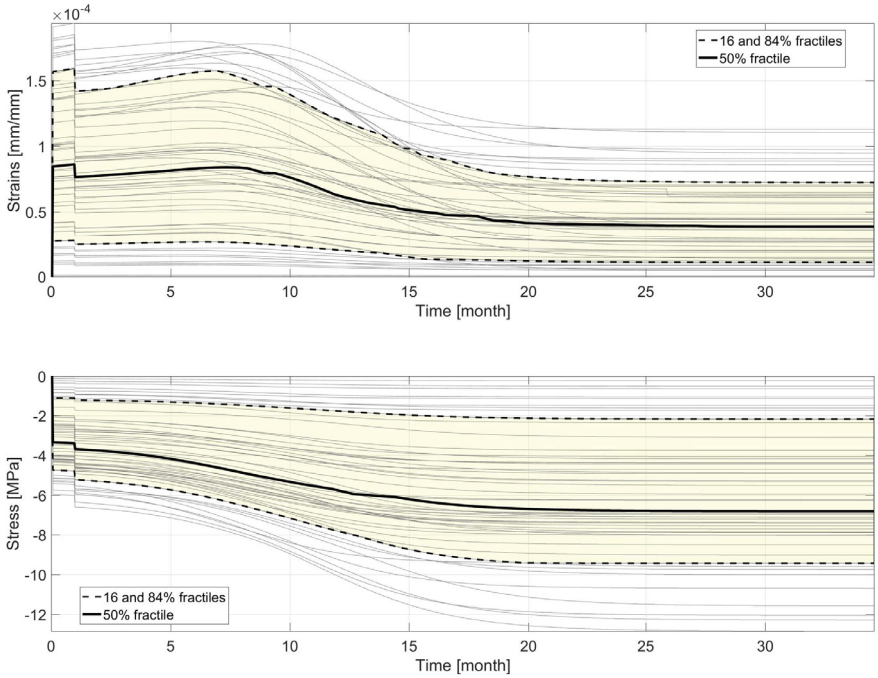

Fig. 3.24. Stress & Strains at Locator # 22, DOF = 2, Coordinates (m)<0.8382, 0.9652, 0.7112>

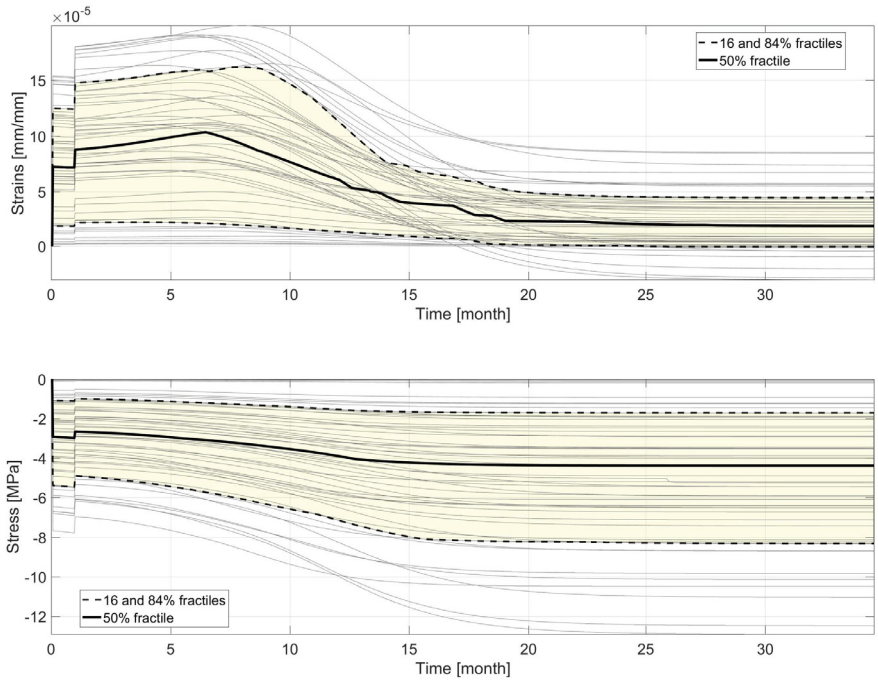

Fig. 3.25. Stress & Strains at Locator # 23, DOF = 2, Coordinates (m)<1.6002, 1.2192, 0.3048>

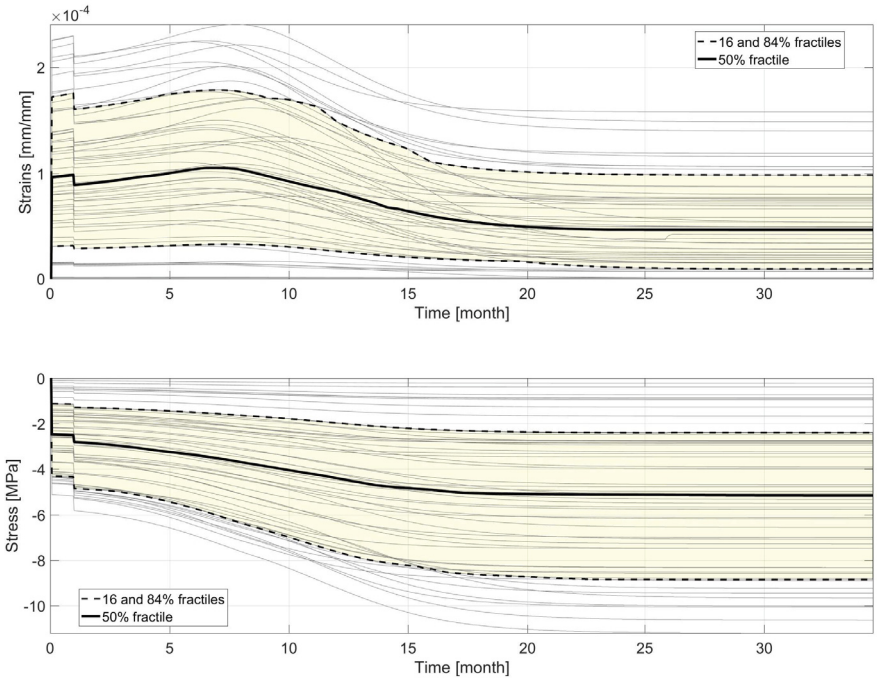

Fig. 3.26. Stress & Strains at Locator # 24, DOF = 2, Coordinates (m)<1.6002, 1.2192,0.7112>

3.2.2 DEMEC

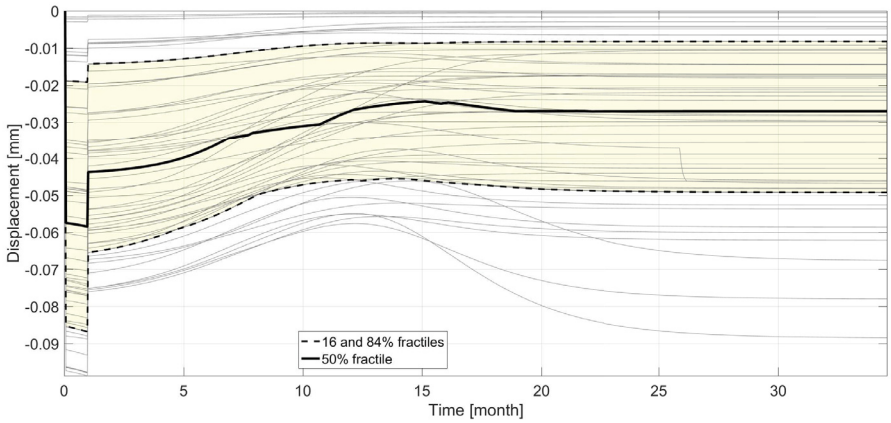

Fig. 3.27. Demec Reading # 1; Between <1.004273, 0.761996, 1.016> and <1.727196, 0.761996, 1.016>

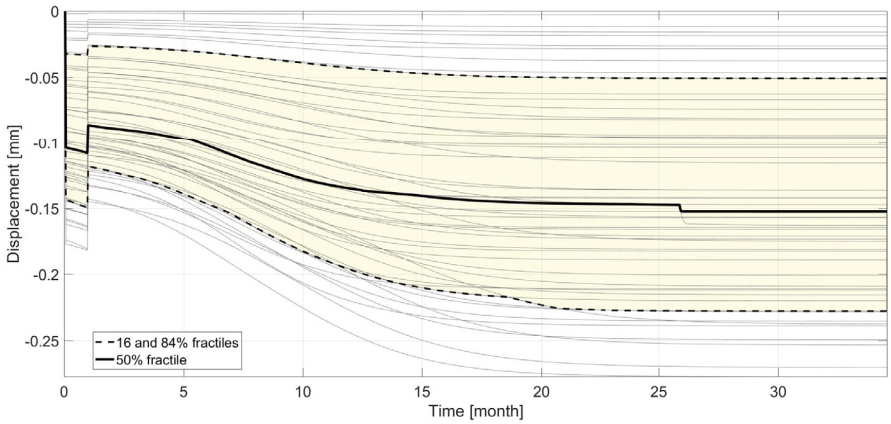

Fig. 3.28. Demec Reading # 2; Between <1.004273, 0.761996, 1.016> and <1.004273, 1.473196, 1.016>

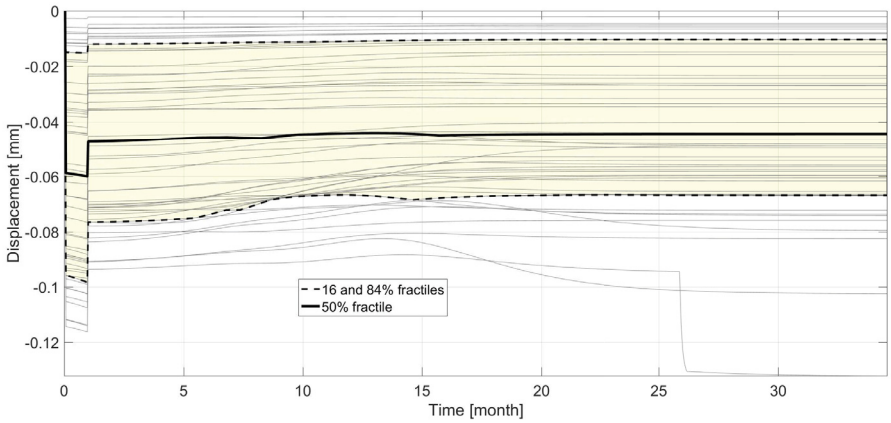

Fig. 3.29. Demec Reading # 3; Between <1.004273, 1.473196, 1.016> and <1.727196, 1.473196, 1.016>

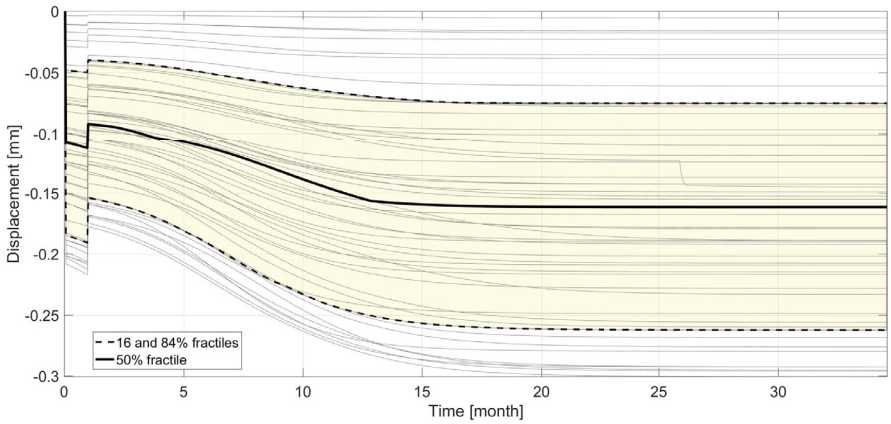

Fig. 3.30. Demec Reading # 4; Between <1.727196, 0.761996, 1.016> and <1.727196, 1.473196, 1.016>

3.2.3 DISPLACEMENTS

Vertical displacement in z direction (fig. 3.31 fig. 3.32) are indeed as easily anticipated, larger in the top than in the bottom due to past bottom support.

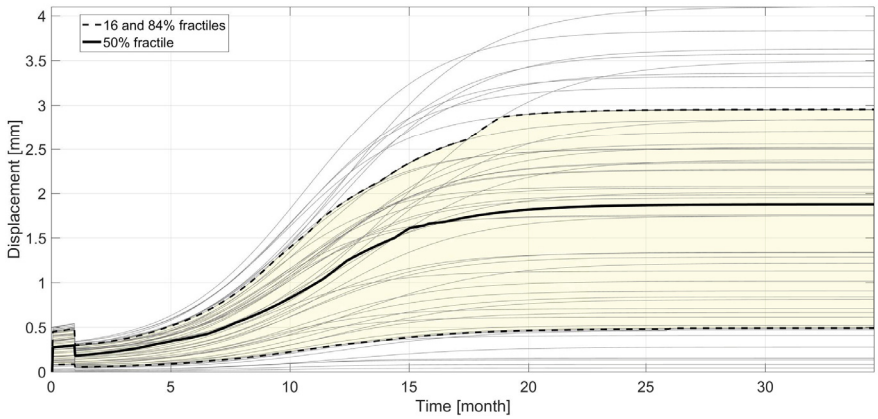

Fig. 3.31. Vertical displacement of top center point.

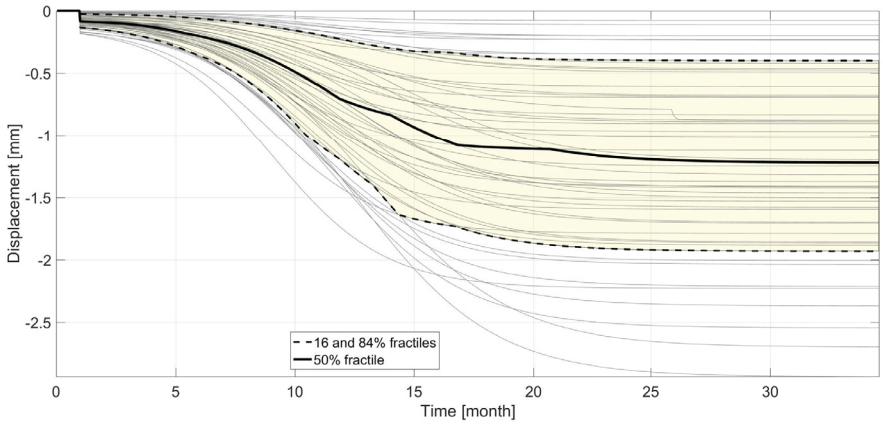

Fig. 3.32. Vertical displacement of bottom center point.

3.2.4 REINFORCEMENTS STRESS AND STRAINS

fig. 3.33 to fig. 3.40 are uncharacteristic. None of them yield, and are all in tension which is expected gven the restrained expansion of the concrete.

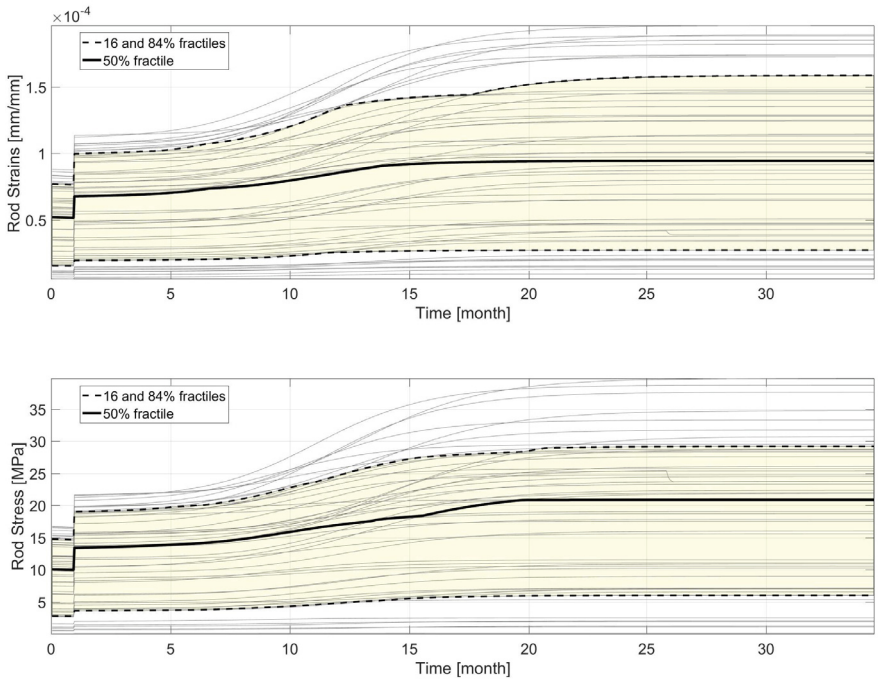

Fig. 3.33. Reinforcement stress and strain at Locator # 1;<1.632, 1.378, 0.0953>

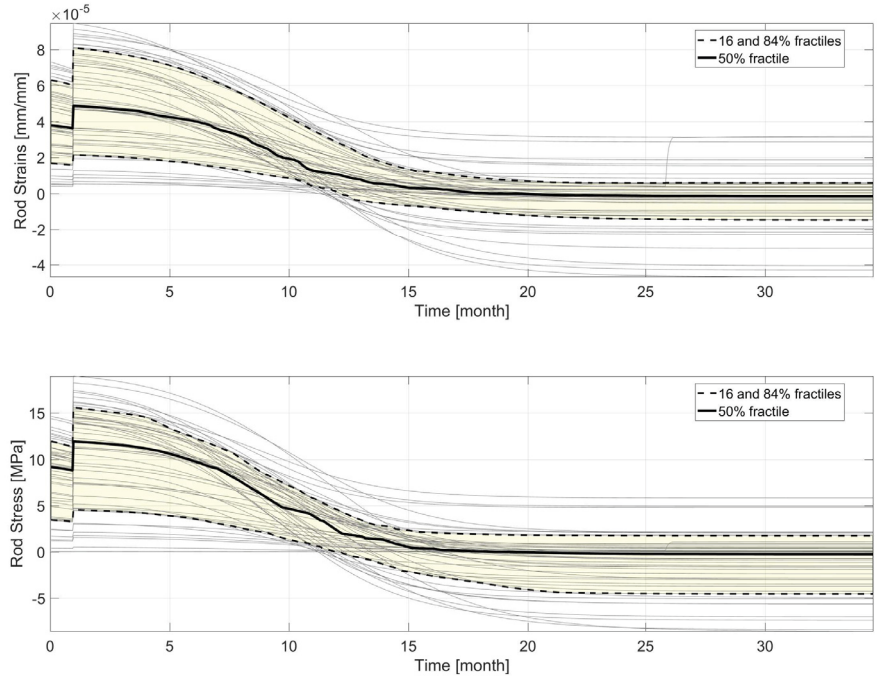

Fig. 3.34. Reinforcement stress and strain at Locator # 2;<2.14, 1.886, 0.0953>

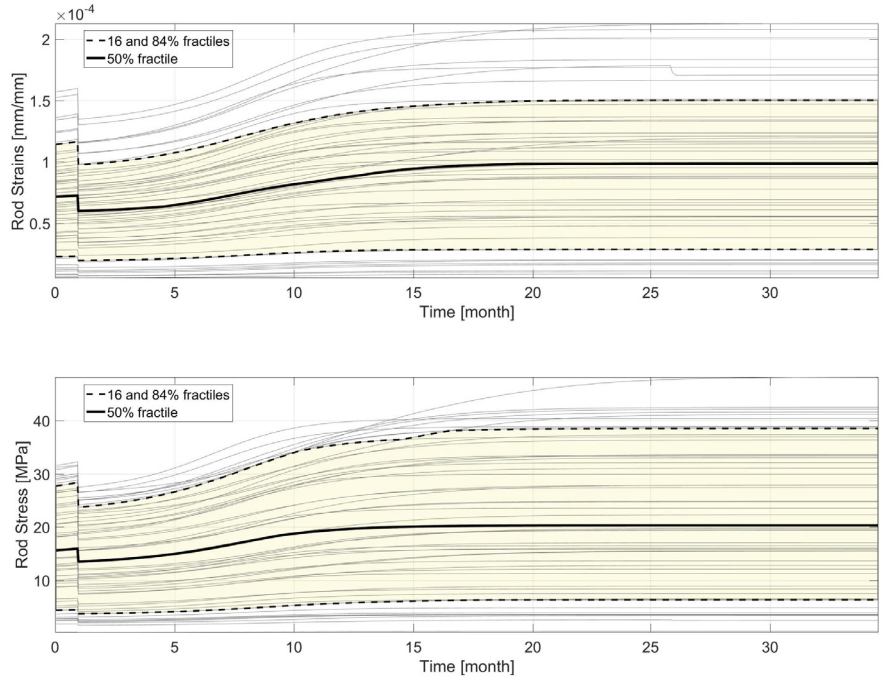

Fig. 3.35. Reinforcement stress and strain at Locator # 3;<1.632, 1.378, 0.9208>

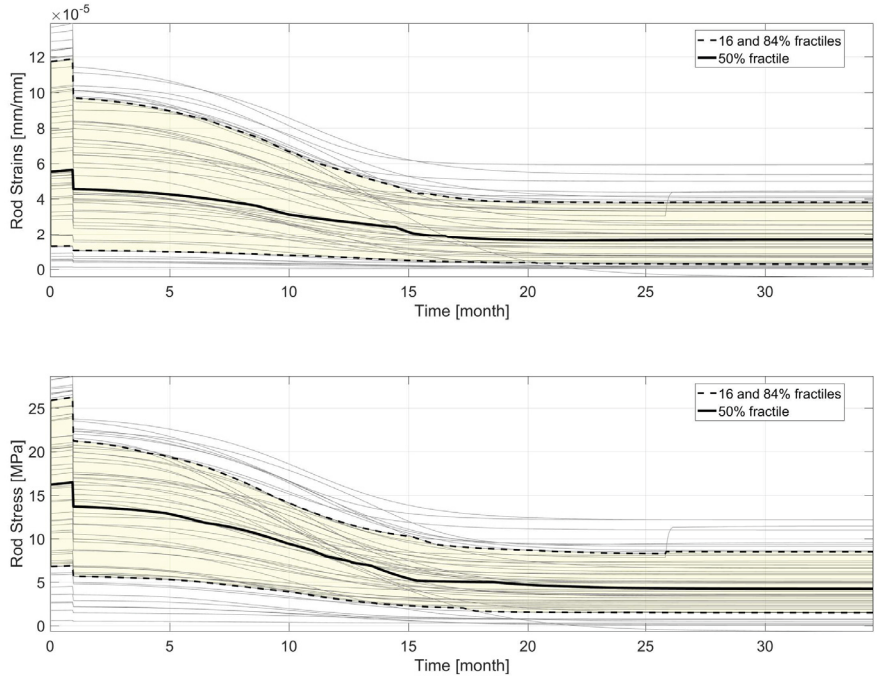

Fig. 3.36. Reinforcement stress and strain at Locator # 4;<2.14, 1.886, 0.9208>

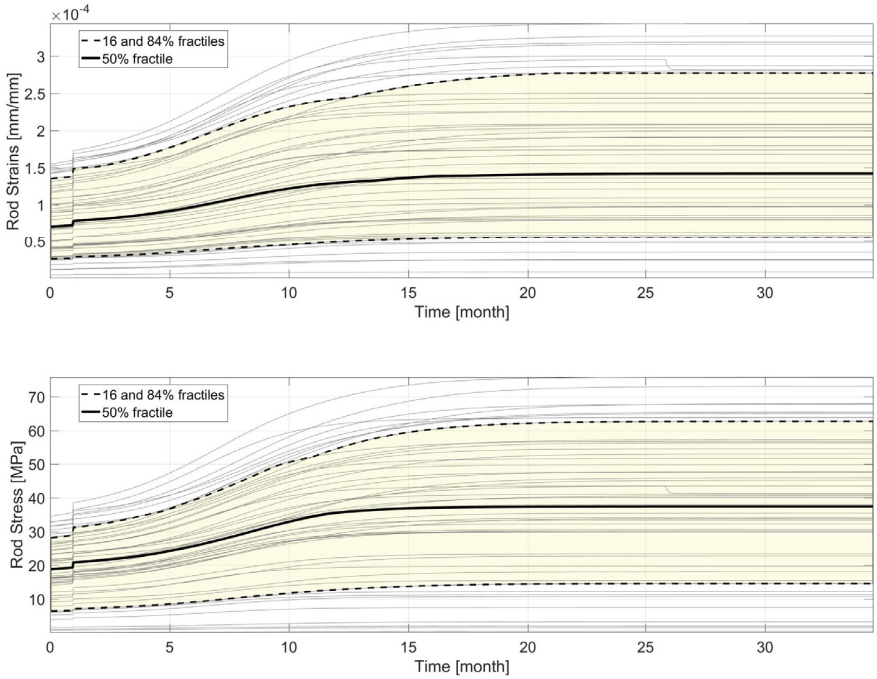

Fig. 3.37. Reinforcement stress and strain at Locator # 5;<1.632, 1.378, 0.1334>

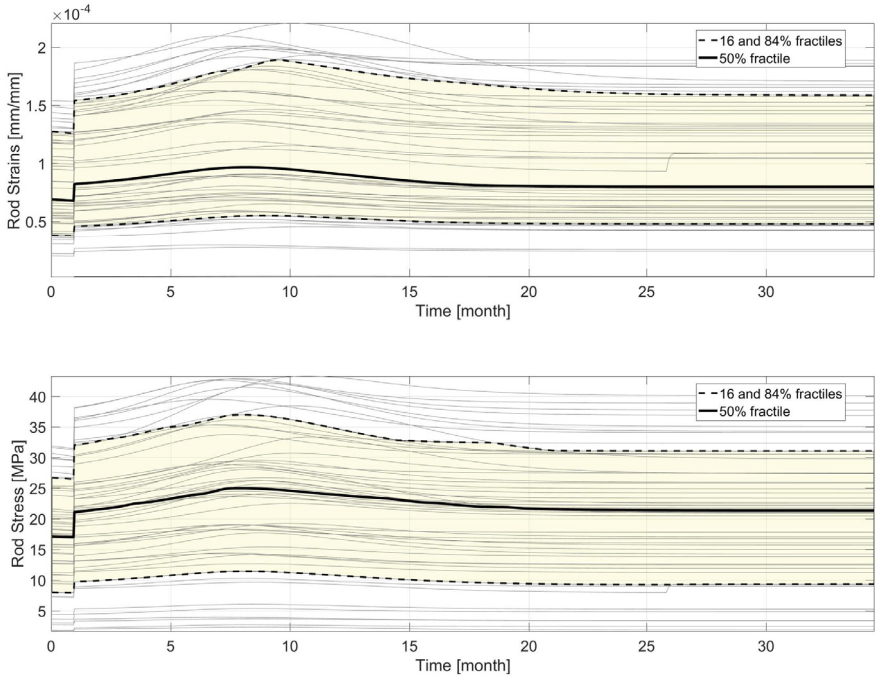

Fig. 3.38. Reinforcement stress and strain at Locator # 6;<2.14, 1.886, 0.1334>

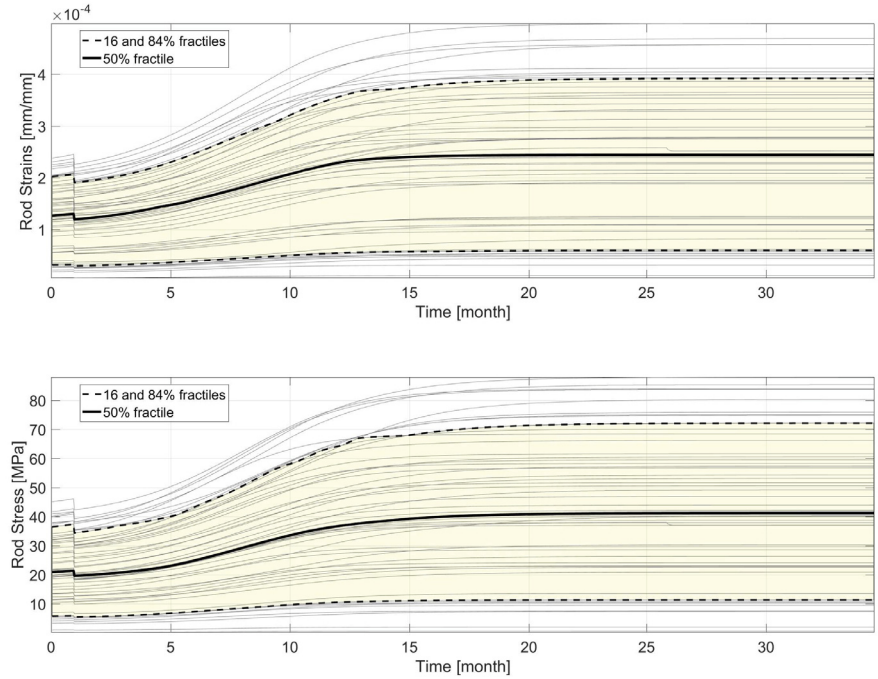

Fig. 3.39. Reinforcement stress and strain at Locator # 7;<1.632, 1.378, 0.8827>

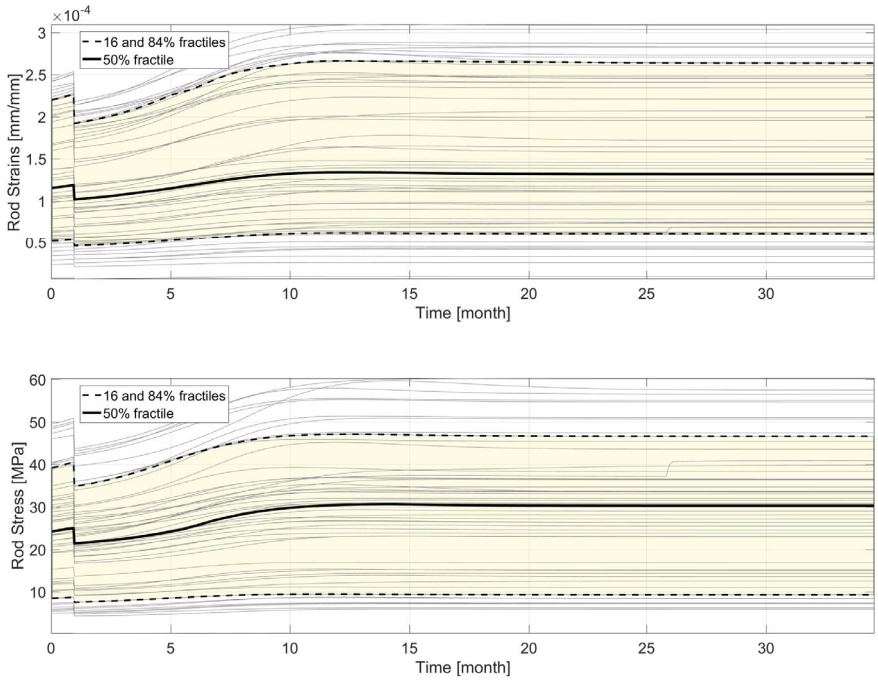

Fig. 3.40. Reinforcement stress and strain at Locator # 8;<2.14, 1.886, 0.8827>

3.3 CONCLUSIONS

A structural model of the large-scale confined ASR specimen currently being tested at the University of Tennessee (Sponsor: U.S. DOE Light Water Reactor Sustainability Program) has been developed using code Merlin, a well-validated code for modeling alkali-silica reaction in concrete structures.

Based on the design drawings provided by the University of Tennessee and the preliminary materials data provided by the University of Alabama, both a deterministic and a probabilistic finite element models were developed in order to provide a âĂŸblindâĂŹ prediction of the future local and structural expansions, strains and stresses at the location of the embedded sensors during a nearly 3-years period.

The obtained estimation will serve as a basis for comparison of the actual monitoring data. In particular, the model will make it possible (1) to detect “anomalous” sensor behavior and engage thorough interpretation if necessary; and (2) to envision the development of monitoring-based updating strategy of the numerical model as an accompanying tool, following the concept of Building information Model.

Bibliography

Bažant, Z. and Becq-Giraudon, E.: 2001, Estimation of fracture energy from basic characteristics of concrete, *in* R. de Borst, J. Mazars, G. Pijaudier-Cabot and J. van Mier (eds), *Fracture Mechanics of Concrete Structures (Proc., FraMCoS-4 Int. Conf., Paris)*, Balkema, pp. 491–Ú495.

Conover, W.J.: 1980, *Practical nonparametric statistics, 2nd ed.*, Wiley, New York.

Iman, R. and Conover, W.: 1982, A distribution-free approach to inducing rank correlation among input variables, *Communications in Statistics-Simulation and Computation* **B11**, 311–334.

Larive, C.: 1998, *Apports Combinés de l'Experimentation et de la Modélisation à la Comprehension del'Alcali-Réaction et de ses Effets Mécaniques*, PhD thesis, *Laboratoire Central des Ponts et Chaussées*, Paris.

Multon, S., Barin, F., Godart, B. and Toutlemonde, F.: 2008, Estimation of the residual expansion of concrete affected by alkali silica reaction, *Journal of Materials in Civil Engineering* **20**, 54–62.

Saouma, V., Martin, R., Hariri-Ardebili, M. and Katayama, T.: 2015, A mathematical model for the kinetics of the alkali-silica chemical reaction, *Cement and Concrete Research* **68**, 184–195.

Appendix A

Data Base & P5.m

Provided with this report is the .mat (binary Matlab) file which contains all simulation results. To facilitate its comprehension, the Matlab code P5.m which generated all the plots in this report is listed.

```
% ==========================================================================
% P5_AAR_mockup.m
% Prepared by: Dr. Mohammad Amin Hariri-Ardebili
% University of Colorado Boulder
% E-mail: moha2643@colorado.edu
% Prepared: September 2016
% ==========================================================================
clear;
close all;
clc;
% GS = 'c:/Program Files/gs/gs9.10/bin/gswin64.exe';
% ==========================================================================
load('Compact_Results.mat');
StartSize  = 1;
SampleSize = 53;
NDisp      = 6;   % Number of displ-base outputs
NStrain    = 24;  % Number of strain-base outputs
NStress    = 24;  % Number of stress-base outputs
NRod       = 8;   % Number of stress-base outputs
ActivePlot = 1;
% ==========================================================================
% Target increments
Target_Inc = [1:1036]/30;
Target_Inc2 = [1:1035]/30;
% Determine the fractiles
% Displacement
for i = 1:NDisp;
Displ_Res_Fractiles(:,1,i) = prctile(Displ_Res(:,:,i), 16, 2);
Displ_Res_Fractiles(:,2,i) = prctile(Displ_Res(:,:,i), 50, 2);
Displ_Res_Fractiles(:,3,i) = prctile(Displ_Res(:,:,i), 84, 2);
end
% Strain
for i = 1:NStrain;
Strain_Res_Fractiles(:,1,i) = prctile(Strain_Res(:,:,i), 16, 2);
Strain_Res_Fractiles(:,2,i) = prctile(Strain_Res(:,:,i), 50, 2);
Strain_Res_Fractiles(:,3,i) = prctile(Strain_Res(:,:,i), 84, 2);
end
```

```
% Stress
for i = 1:NStress;
Stress_Res_Fractiles(:,1,i) = prctile(Stress_Res(:,:,i), 16, 2);
Stress_Res_Fractiles(:,2,i) = prctile(Stress_Res(:,:,i), 50, 2);
Stress_Res_Fractiles(:,3,i) = prctile(Stress_Res(:,:,i), 84, 2);
end
% Strain
for i = 1:NRod;
Rod_Strain_Res_Fractiles(:,1,i) = prctile(Rod_Strain_Res(:,:,i), 16, 2);
Rod_Strain_Res_Fractiles(:,2,i) = prctile(Rod_Strain_Res(:,:,i), 50, 2);
Rod_Strain_Res_Fractiles(:,3,i) = prctile(Rod_Strain_Res(:,:,i), 84, 2);
end
% Stress
for i = 1:NRod;
Rod_Stress_Res_Fractiles(:,1,i) = prctile(Rod_Stress_Res(:,:,i), 16, 2);
Rod_Stress_Res_Fractiles(:,2,i) = prctile(Rod_Stress_Res(:,:,i), 50, 2);
Rod_Stress_Res_Fractiles(:,3,i) = prctile(Rod_Stress_Res(:,:,i), 84, 2);
end

% ========================================================================
% plot
%% ----------------------------- Displacement
if ActivePlot == 0;
for i = 1:1; % NDisp;
fs = 18; % FontSize
scrsz = get(0,'ScreenSize'); % Screen size
hf1 = figure('Position',[1 scrsz(4)/3 scrsz(3)/1.8 scrsz(4)/2.0],'Name','Plots','NumberTitle','off');
set(gca,'FontSize',fs);
% Plot shaded area between fractiles
XX = [Target_Inc, fliplr(Target_Inc)];
YY = [1000* Displ_Res_Fractiles(:,3,i)', fliplr(1000* Displ_Res_Fractiles(:,1,i)')];
fill(XX,YY,'y');
alpha(0.1);
hold on
% plot individual lines
for j = StartSize:1:SampleSize;
h0 = plot(Target_Inc, 1000* Displ_Res(:,j,i), '-', 'Color', [0.5, 0.5, 0.5], 'LineWidth',0.5, 'MarkerSize',6);
hold on
end
% plot three fractiles
h1 = plot(Target_Inc, 1000* Displ_Res_Fractiles(:,1,i), 'k--', 'MarkerEdgeColor','b', 'MarkerFaceColor','w', 'LineWidth',2.0, 'MarkerSize',6);
hold on
h2 = plot(Target_Inc, 1000* Displ_Res_Fractiles(:,2,i), 'k-', 'MarkerEdgeColor','b', 'MarkerFaceColor','w', 'LineWidth',3.0, 'MarkerSize',6);
hold on
h3= plot(Target_Inc, 1000* Displ_Res_Fractiles(:,3,i), 'k--', 'MarkerEdgeColor','b', 'MarkerFaceColor','w', 'LineWidth',2.0, 'MarkerSize',6);
% plot options
legend([h1 h2], '16 and 84% fractiles','50% fractile', 'Location', 'Best')
xlabel('Time [month]','FontSize',18,'FontName','Arial');
ylabel('Displacement [mm]','FontSize',18,'FontName','Arial');
xlim([0 max(Target_Inc)]);
ylim([-inf inf]);
```

```
grid on;
box on;
% Save as .eps
set(gca,'FontSize',fs);
set(gcf,'PaperPositionMode','auto');
FileName=['./Figs/Dem' num2str(i) '.eps'];
print(FileName,'-depsc');
%     eps2pdf(FileName,GS,0);
end
end
%% ---------------------------- Strain and Stress as sub-plots
if ActivePlot == 0;
for i = 1:1; % NStrain;
fs = 18; % FontSize
scrsz = get(0,'ScreenSize'); % Screen size
hf2 = figure('Position',[1 scrsz(4)/10 scrsz(3)/1.8 scrsz(4)/1.2],'Name','Plots','NumberTitle','off');
set(gca,'FontSize',fs);
% ------------------------- subplot(1):strain
subplot(2,1,1)
% Plot shaded area between fractiles
XX = [Target_Inc, fliplr(Target_Inc)];
YY = [Strain_Res_Fractiles(:,3,i)', fliplr(Strain_Res_Fractiles(:,1,i)')];
fill(XX,YY,'y');
alpha(0.1);
hold on
% plot individual lines
for j = StartSize:1:SampleSize;
h0 = plot(Target_Inc, Strain_Res(:,j,i), '-', 'Color', [0.5, 0.5, 0.5], 'LineWidth',0.5, 'MarkerSize',6);
hold on
end
% plot three fractiles
h1 = plot(Target_Inc, Strain_Res_Fractiles(:,1,i), 'k--', 'MarkerEdgeColor','b', 'MarkerFaceColor','w', 'LineWidth',2.0, 'MarkerSize',6);
hold on
h2 = plot(Target_Inc, Strain_Res_Fractiles(:,2,i), 'k-', 'MarkerEdgeColor','b', 'MarkerFaceColor','w', 'LineWidth',3.0, 'MarkerSize',6);
hold on
h3= plot(Target_Inc, Strain_Res_Fractiles(:,3,i), 'k--', 'MarkerEdgeColor','b', 'MarkerFaceColor','w', 'LineWidth',2.0, 'MarkerSize',6);
% plot options
legend([h1 h2], '16 and 84% fractiles','50% fractile', 'Location', 'Best')
xlabel('Time [month]','FontSize',18,'FontName','Arial');
ylabel('Strains [mm/mm]','FontSize',18,'FontName','Arial');
xlim([0 max(Target_Inc)]);
ylim([-inf inf]);
grid on;
box on;
set(gca,'FontSize',fs);
% ------------------------- subplot(2):stress
subplot(2,1,2)
% Plot shaded area between fractiles
XX = [Target_Inc, fliplr(Target_Inc)];
YY = [Stress_Res_Fractiles(:,3,i)', fliplr(Stress_Res_Fractiles(:,1,i)')];
fill(XX,YY,'y');
```

```
alpha(0.1);
hold on
% plot individual lines
for j = StartSize:1:SampleSize;
h0 = plot(Target_Inc, Stress_Res(:,j,i), '-', 'Color', [0.5, 0.5, 0.5], 'LineWidth'
    ,0.5, 'MarkerSize',6);
hold on
end
% plot three fractiles
h1 = plot(Target_Inc, Stress_Res_Fractiles(:,1,i), 'k--', 'MarkerEdgeColor','b', '
    MarkerFaceColor','w', 'LineWidth',2.0, 'MarkerSize',6);
hold on
h2 = plot(Target_Inc, Stress_Res_Fractiles(:,2,i), 'k-', 'MarkerEdgeColor','b', '
    MarkerFaceColor','w', 'LineWidth',3.0, 'MarkerSize',6);
hold on
h3= plot(Target_Inc, Stress_Res_Fractiles(:,3,i), 'k--', 'MarkerEdgeColor','b', '
    MarkerFaceColor','w', 'LineWidth',2.0, 'MarkerSize',6);
% plot options
legend([h1 h2], '16 and 84% fractiles','50% fractile', 'Location', 'Best')
xlabel('Time [month]','FontSize',18,'FontName','Arial');
ylabel('Stress [MPa]','FontSize',18,'FontName','Arial');
xlim([0 max(Target_Inc)]);
ylim([-inf inf]);
grid on;
box on;
% Save as .eps
set(gca,'FontSize',fs);
set(gcf,'PaperPositionMode','auto');
FileName=['./Figs/SS' num2str(i) '.eps'];
print(FileName,'-depsc');
%     eps2pdf(FileName,GS,0);
end
end
%% ---------------------------- Strain
if ActivePlot == 0;
for i = 1:NStrain; % NStrain;
fs = 18; % FontSize
scrsz = get(0,'ScreenSize'); % Screen size
hf2 = figure('Position',[1 scrsz(4)/3 scrsz(3)/2.0 scrsz(4)/2.0],'Name','Plots','
    NumberTitle','off');
set(gca,'FontSize',fs);
% Plot shaded area between fractiles
XX = [Target_Inc, fliplr(Target_Inc)];
YY = [Strain_Res_Fractiles(:,3,i)', fliplr(Strain_Res_Fractiles(:,1,i)')];
fill(XX,YY,'y');
alpha(0.1);
hold on
% plot individual lines
for j = StartSize:1:SampleSize;
h0 = plot(Target_Inc, Strain_Res(:,j,i), '-', 'Color', [0.5, 0.5, 0.5], 'LineWidth'
    ,0.5, 'MarkerSize',6);
hold on
end
% plot three fractiles
h1 = plot(Target_Inc, Strain_Res_Fractiles(:,1,i), 'b-', 'MarkerEdgeColor','b', '
    MarkerFaceColor','w', 'LineWidth',2.0, 'MarkerSize',6);
```

```
hold on
h2 = plot(Target_Inc, Strain_Res_Fractiles(:,2,i), 'k-', 'MarkerEdgeColor','b', 'MarkerFaceColor','w', 'LineWidth',2.0, 'MarkerSize',6);
hold on
h3= plot(Target_Inc, Strain_Res_Fractiles(:,3,i), 'r-', 'MarkerEdgeColor','b', 'MarkerFaceColor','w', 'LineWidth',2.0, 'MarkerSize',6);
% plot options
legend([h0 h1 h2 h3], 'Individuals', 'Mean - STD','Mean', 'Mean + STD', 'Location', 'Best')
xlabel('Time [month]','FontSize',18,'FontName','Arial');
ylabel('Strains [mm/mm]','FontSize',18,'FontName','Arial');
xlim([0 max(Target_Inc)]);
ylim([-inf inf]);
grid on;
box on;
% Save as .eps
set(gca,'FontSize',fs);
set(gcf,'PaperPositionMode','auto');
FileName=['./Figs/Strain' num2str(i) '.eps'];
print(FileName,'-depsc');
%     eps2pdf(FileName,GS,0);
end
end
%% ---------------------------- Stress
if ActivePlot == 0;
for i = 1:NStress; % NStress;
fs = 18; % FontSize
scrsz = get(0,'ScreenSize'); % Screen size
hf2 = figure('Position',[1 scrsz(4)/3 scrsz(3)/2.0 scrsz(4)/2.0],'Name','Plots','NumberTitle','off');
set(gca,'FontSize',fs);
% Plot shaded area between fractiles
XX = [Target_Inc, fliplr(Target_Inc)];
YY = [Stress_Res_Fractiles(:,3,i)', fliplr(Stress_Res_Fractiles(:,1,i)')];
fill(XX,YY,'y');
alpha(0.1);
hold on
% plot individual lines
for j = StartSize:1:SampleSize;
h0 = plot(Target_Inc, Stress_Res(:,j,i), '-', 'Color', [0.5, 0.5, 0.5], 'LineWidth',0.5, 'MarkerSize',6);
hold on
end
% plot three fractiles
h1 = plot(Target_Inc, Stress_Res_Fractiles(:,1,i), 'b-', 'MarkerEdgeColor','b', 'MarkerFaceColor','w', 'LineWidth',2.0, 'MarkerSize',6);
hold on
h2 = plot(Target_Inc, Stress_Res_Fractiles(:,2,i), 'k-', 'MarkerEdgeColor','b', 'MarkerFaceColor','w', 'LineWidth',2.0, 'MarkerSize',6);
hold on
h3= plot(Target_Inc, Stress_Res_Fractiles(:,3,i), 'r-', 'MarkerEdgeColor','b', 'MarkerFaceColor','w', 'LineWidth',2.0, 'MarkerSize',6);
% plot options
legend([h0 h1 h2 h3], 'Individuals', 'Mean - STD','Mean', 'Mean + STD', 'Location', 'Best')
xlabel('Time [month]','FontSize',18,'FontName','Arial');
```

```
ylabel('Stress [MPa]','FontSize',18,'FontName','Arial');
xlim([0 max(Target_Inc)]);
ylim([-inf inf]);
grid on;
box on;
% Save as .eps
set(gca,'FontSize',fs);
set(gcf,'PaperPositionMode','auto');
FileName=['./Figs/Stress' num2str(i) '.eps'];
print(FileName,'-depsc');
%     eps2pdf(FileName,GS,0);
end
end
%% ---------------------------- Strain and Stress as sub-plots
if ActivePlot == 1;
for i = 1:1; % NRod;
fs = 18; % FontSize
scrsz = get(0,'ScreenSize'); % Screen size
hf2 = figure('Position',[1 scrsz(4)/10 scrsz(3)/1.8 scrsz(4)/1.2],'Name','Plots','NumberTitle','off');
set(gca,'FontSize',fs);
% ------------------------- subplot(1):strain
subplot(2,1,1)
% Plot shaded area between fractiles
XX = [Target_Inc2, fliplr(Target_Inc2)];
YY = [Rod_Strain_Res_Fractiles(:,3,i)', fliplr(Rod_Strain_Res_Fractiles(:,1,i)')];
fill(XX,YY,'y');
alpha(0.1);
hold on
% plot individual lines
for j = StartSize:1:SampleSize;
h0 = plot(Target_Inc2, Rod_Strain_Res(:,j,i), '-', 'Color', [0.5, 0.5, 0.5], 'LineWidth',0.5, 'MarkerSize',6);
hold on
end
% plot three fractiles
h1 = plot(Target_Inc2, Rod_Strain_Res_Fractiles(:,1,i), 'k--', 'MarkerEdgeColor','b', 'MarkerFaceColor','w', 'LineWidth',2.0, 'MarkerSize',6);
hold on
h2 = plot(Target_Inc2, Rod_Strain_Res_Fractiles(:,2,i), 'k-', 'MarkerEdgeColor','b', 'MarkerFaceColor','w', 'LineWidth',3.0, 'MarkerSize',6);
hold on
h3= plot(Target_Inc2, Rod_Strain_Res_Fractiles(:,3,i), 'k--', 'MarkerEdgeColor','b', 'MarkerFaceColor','w', 'LineWidth',2.0, 'MarkerSize',6);
% plot options
legend([h1 h2], '16 and 84% fractiles','50% fractile', 'Location', 'Best')
xlabel('Time [month]','FontSize',18,'FontName','Arial');
ylabel('Rod Strains [mm/mm]','FontSize',18,'FontName','Arial');
xlim([0 max(Target_Inc2)]);
ylim([-inf inf]);
grid on;
box on;
set(gca,'FontSize',fs);
% ------------------------- subplot(2):stress
subplot(2,1,2)
% Plot shaded area between fractiles
```

```
XX = [Target_Inc2, fliplr(Target_Inc2)];
YY = [Rod_Stress_Res_Fractiles(:,3,i)', fliplr(Rod_Stress_Res_Fractiles(:,1,i)')];
fill(XX,YY,'y');
alpha(0.1);
hold on
% plot individual lines
for j = StartSize:1:SampleSize;
h0 = plot(Target_Inc2, Rod_Stress_Res(:,j,i), '-', 'Color', [0.5, 0.5, 0.5], 'LineWidth',0.5, 'MarkerSize',6);
hold on
end
% plot three fractiles
h1 = plot(Target_Inc2, Rod_Stress_Res_Fractiles(:,1,i), 'k--', 'MarkerEdgeColor','b', 'MarkerFaceColor','w', 'LineWidth',2.0, 'MarkerSize',6);
hold on
h2 = plot(Target_Inc2, Rod_Stress_Res_Fractiles(:,2,i), 'k-', 'MarkerEdgeColor','b', 'MarkerFaceColor','w', 'LineWidth',3.0, 'MarkerSize',6);
hold on
h3= plot(Target_Inc2, Rod_Stress_Res_Fractiles(:,3,i), 'k--', 'MarkerEdgeColor','b', 'MarkerFaceColor','w', 'LineWidth',2.0, 'MarkerSize',6);
% plot options
legend([h1 h2], '16 and 84% fractiles','50% fractile', 'Location', 'Best')
xlabel('Time [month]','FontSize',18,'FontName','Arial');
ylabel('Rod Stress [MPa]','FontSize',18,'FontName','Arial');
xlim([0 max(Target_Inc2)]);
ylim([-inf inf]);
grid on;
box on;
% Save as .eps
set(gca,'FontSize',fs);
set(gcf,'PaperPositionMode','auto');
FileName=['./Figs/Rod' num2str(i) '.eps'];
print(FileName,'-depsc');
%     eps2pdf(FileName,GS,0);
end
end
%% ---------------------------- Rod Strain
if ActivePlot == 0;
for i = 1:NRod; % NRod;
fs = 18; % FontSize
scrsz = get(0,'ScreenSize'); % Screen size
hf2 = figure('Position',[1 scrsz(4)/3 scrsz(3)/2.0 scrsz(4)/2.0],'Name','Plots','NumberTitle','off');
set(gca,'FontSize',fs);
% Plot shaded area between fractiles
XX = [Target_Inc2, fliplr(Target_Inc2)];
YY = [Rod_Strain_Res_Fractiles(:,3,i)', fliplr(Rod_Strain_Res_Fractiles(:,1,i)')];
fill(XX,YY,'y');
alpha(0.1);
hold on
% plot individual lines
for j = StartSize:1:SampleSize;
h0 = plot(Target_Inc2, Rod_Strain_Res(:,j,i), '-', 'Color', [0.5, 0.5, 0.5], 'LineWidth',0.5, 'MarkerSize',6);
hold on
end
```

```
% plot three fractiles
h1 = plot(Target_Inc2, Rod_Strain_Res_Fractiles(:,1,i), 'b-', 'MarkerEdgeColor','b', 'MarkerFaceColor','w', 'LineWidth',2.0, 'MarkerSize',6);
hold on
h2 = plot(Target_Inc2, Rod_Strain_Res_Fractiles(:,2,i), 'k-', 'MarkerEdgeColor','b', 'MarkerFaceColor','w', 'LineWidth',2.0, 'MarkerSize',6);
hold on
h3= plot(Target_Inc2, Rod_Strain_Res_Fractiles(:,3,i), 'r-', 'MarkerEdgeColor','b', 'MarkerFaceColor','w', 'LineWidth',2.0, 'MarkerSize',6);
% plot options
legend([h0 h1 h2 h3], 'Individuals', 'Mean - STD','Mean', 'Mean + STD', 'Location', 'Best')
xlabel('Time [month]','FontSize',18,'FontName','Arial');
ylabel('Rod Strains [mm/mm]','FontSize',18,'FontName','Arial');
xlim([0 max(Target_Inc2)]);
ylim([-inf inf]);
grid on;
box on;
% Save as .eps
set(gca,'FontSize',fs);
set(gcf,'PaperPositionMode','auto');
FileName=['./Figs/RodStrain' num2str(i) '.eps'];
print(FileName,'-depsc');
%     eps2pdf(FileName,GS,0);
end
end
%% ----------------------------- Rod stress
if ActivePlot == 0;
for i = 1:NRod; % NRod;
fs = 18; % FontSize
scrsz = get(0,'ScreenSize'); % Screen size
hf2 = figure('Position',[1 scrsz(4)/3 scrsz(3)/2.0 scrsz(4)/2.0],'Name','Plots','NumberTitle','off');
set(gca,'FontSize',fs);
% Plot shaded area between fractiles
XX = [Target_Inc2, fliplr(Target_Inc2)];
YY = [Rod_Stress_Res_Fractiles(:,3,i)', fliplr(Rod_Stress_Res_Fractiles(:,1,i)')];
fill(XX,YY,'y');
alpha(0.1);
hold on
% plot individual lines
for j = StartSize:1:SampleSize;
h0 = plot(Target_Inc2, Rod_Stress_Res(:,j,i), '-', 'Color', [0.5, 0.5, 0.5], 'LineWidth',0.5, 'MarkerSize',6);
hold on
end
% plot three fractiles
h1 = plot(Target_Inc2, Rod_Stress_Res_Fractiles(:,1,i), 'b-', 'MarkerEdgeColor','b', 'MarkerFaceColor','w', 'LineWidth',2.0, 'MarkerSize',6);
hold on
h2 = plot(Target_Inc2, Rod_Stress_Res_Fractiles(:,2,i), 'k-', 'MarkerEdgeColor','b', 'MarkerFaceColor','w', 'LineWidth',2.0, 'MarkerSize',6);
hold on
h3= plot(Target_Inc2, Rod_Stress_Res_Fractiles(:,3,i), 'r-', 'MarkerEdgeColor','b', 'MarkerFaceColor','w', 'LineWidth',2.0, 'MarkerSize',6);
% plot options
```

```
legend([h0 h1 h2 h3], 'Individuals', 'Mean - STD','Mean', 'Mean + STD', 'Location', 'Best')
xlabel('Time [month]','FontSize',18,'FontName','Arial');
ylabel('Rod Stress [MPa]','FontSize',18,'FontName','Arial');
xlim([0 max(Target_Inc2)]);
ylim([-inf inf]);
grid on;
box on;
% Save as .eps
set(gca,'FontSize',fs);
set(gcf,'PaperPositionMode','auto');
FileName=['./Figs/Rod_Stress' num2str(i) '.eps'];
print(FileName,'-depsc');
%     eps2pdf(FileName,GS,0);
end
end
```